2011

Modeling the population effects of hypoxia on Atlantic croaker (Micropogonias undulatus) in the northwestern Gulf of Mexico

Sean Brandon Creekmore
Louisiana State University and Agricultural and Mechanical College

MODELING THE POPULATION EFFECTS OF HYPOXIA ON ATLANTIC CROAKER (MICROPOGONIAS UNDULATUS) IN THE NORTHWESTERN GULF OF MEXICO

A Thesis
Submitted to the Graduate Faculty of the
Louisiana State University and
Agricultural and Mechanical College
in partial fulfillment of the
requirements for the degree of
Master of Science

in

The Department of Oceanography and Coastal Sciences

by
Sean Brandon Creekmore
B.S., University of West Florida, 2007
August 2011

ACKNOWLEDGEMENTS

Funding for this project was provided by the National Oceanic and Atmospheric Administration, Center for Sponsored Coastal Ocean Research (CSCOR), NGOMEX06 grant number NA06NOS4780131 and NGOMEX09 grant number NA09NOS4780179 awarded to the University of Texas. I would like to thank Dr. Kenneth Rose for giving me the opportunity to take part in a collaborative effort to study the effects of hypoxia on fish populations. His guidance, unending patience, and constant encouragement were invaluable during this challenging, rewarding endeavor. I want to convey my sincere gratitude to Drs. Peter Thomas, Kevin Craig, Md Rahman, and Rachael Miller-Neilan whose hard work and expertise really made this research possible; it has been a real privilege working them. I would also like to thank my committee members Drs. Dubravko Justic and Joseph Powers for generously offering their time and assistance, their feed-back on my manuscript is greatly appreciated. Finally, I would like to thank my wife, whose love and support gave me the fortitude to persevere.

TABLE OF CONTENTS

Acknowledgements ii

Abstract iv

Introduction 1
Hypoxia and Croaker in the NWGOM 4

Methods 7
Description of the Model 7
Overview 7
Grid Configuration and Environmental Variables 7
Development and Growth 13
Mortality 18
Reproduction 19
Movement 21
Exposure and Effects of Hypoxia 23
Numerics 25
Initial Conditions 27
Design of Simulations 27
Calibration 27
Hypoxia Effects 30
Sensitivity Analysis 31

Results 34
Calibration 34
Hypoxia Effects: Mild, Intermediate, and Severe 41
Hypoxia Effects: Time Series Simulations 47
Sensitivity Analysis 49

Discussion 51
Effects of Hypoxia 51
Some Model Strengths and Weaknesses 54
Future Directions 56

Literature Cited 59

Appendix A: Derivation of the Mild, Moderate, and Severe Hypoxia Maps 66

Appendix B: Overview of the Bioenergetics Model 67

Vita 68

ABSTRACT

The northwestern Gulf of Mexico currently experiences a large hypoxic area ("dead zone") during the summer. While the local effects of hypoxia on organisms have been documented, the population-level effects are largely unknown. I developed a spatially-explicit, individual-based model to analyze how hypoxia effects on Atlantic croaker reproduction, growth, and mortality in the northwestern Gulf of Mexico could lead to population-level responses. The model follows the hourly growth, mortality, reproduction, and movement of individuals on a 300 x 800 spatial grid of 1 km^2 cells for 100 years. Chlorophyll-a concentration, water temperature, and dissolved oxygen were specified daily for each grid cell for an average year, which was repeated every year. A bioenergetics model was used to represent growth, mortality was assumed age- and size-dependent, and the movement behavior of juveniles and adults was modeled as an unconditioned response to external cues (kinesis) coupled with a neighborhood search algorithm that emulated hypoxia avoidance. Hypoxia effects were imposed using vitality-repair submodels that convert time-varying exposures to reduced hourly growth, increased hourly mortality, and reduced annual fecundity. Results showed that 80 years of either mild or intermediate hypoxia produced small reductions in population abundance, while severe hypoxia caused a 31% reduction in long-term population abundance. The response to severe hypoxia was added age-1 and age-2 daily mortality (8-9%) and a 5% average reduction in eggs per individual. Relatively few individuals (5%) were exposed each hour but many individuals (20-40%) experienced at least one hour of low DO each year. The effects slowly built up in the model over years; population abundance slowly declined for 40 years before the 31% reduction was realized. Under more realistic hypoxia conditions of mild, intermediate, and severe hypoxia years occurring in proportion to their historical frequency, the model predicted an 18-29%

decrease in the long-term population abundance. Sensitivity analysis showed hypoxia effects via reduced growth were small, and aspects of avoidance behavior were important in determining the population response. I discuss the strengths and weaknesses of the modeling, and future plans for refining the analysis based on data from ongoing field and laboratory studies.

INTRODUCTION

Anthropogenic eutrophication is increasing in coastal waters, and has been implicated in causing changes to the ecological structure and functioning in semi-enclosed and coastal marine systems (Diaz & Rosenberg 2008). Ecosystem responses to eutrophication include: shifts in energy flow patterns within the food web, changes in phytoplankton community composition, declines in fish habitat quality, and increases in harmful algal blooms (Cloern 2001, Rabalais et al. 2002). Eutrophication is often, but not always, associated with increasing frequency and duration of hypoxic events that can have negative effects on fish (Cloern 2001, Breitburg 2002). Increased nutrient supplies can also supplement secondary production, thereby increasing fish productivity (Grimes 2001, Nixon & Buckley 2002, Kemp et al. 2005).

Reducing nutrient loadings in large systems incurs high monetary costs, and thus knowing the likely consequences of reduced nutrient loadings on the ecosystem, especially fish, is critical to proper decision-making and public policy formulation (Conley et al., 2009). Management actions to reduce nutrient loadings are partially justified by the purported decrease in hypoxia that may result. While there is no doubt that reducing hypoxia benefits sessile species and has positive local effects on aquatic fauna, there is little direct, quantitative evidence that reducing hypoxia has positive population level effects on coastal fish species (Rose et al. 2009).

Caddy (1993) proposed a conceptual model about how eutrophication and hypoxia affect fish production. Caddy suggested ecosystems will reach a point where the negative effects of increasing enrichment (including hypoxia) will result in declines of demersal and, eventually, pelagic fish species. In a subsequent paper, Caddy (2000) used several case studies (e.g., Black Sea, Baltic Sea) to illustrate how nutrient loadings and hypoxia affect fish populations. However, Brietburg et al. (2009a) analyzed the landings, nutrient loadings, and hypoxia of 12

ecosystems and concluded "It is difficult to find compelling evidence for negative effects of hypoxia on fisheries for mobile species even in systems with extensive and persistent oxygen depletion if system-wide conditions and total landings are the focus of analyses." Except for a few systems, the quantitative evidence for the negative effects of hypoxia on fish populations described in Caddy's conceptual model is limited.

Low DO and hypoxia clearly have detrimental effects on individual fish and on small spatial and temporal scales (i.e., localized effects). For example, laboratory experiments have shown low DO can alter foraging behavior (Pihl et al. 1992, Baustian et al. 2009), reduce growth rate (McNatt and Rice 2004, Stierhoff et al. 2006), affect sex differentiation (Shang et al.2006), and result in reproductive impairment (Thomas et al. 2007, Murphy et al. 2009, Cheek et al. 2009). In ecological studies, low DO has been implicated in causing mass mortality (Thronson and Quigg 2008, McAllen et al. 2009), reducing recruitment (Breitburg 1992, Köster et al. 2005), displacing individuals from preferred habitat (Craig and Crowder 2005, Eby et al. 2005, Tyler and Targett 2007, Chan et al. 2008, Hazen et al. 2009, Switzer et al. 2009), and causing a shift in the system from demersal to pelagic species (de Leiva Moreno et al. 2000, Chesney and Baltz 2001). How these effects relate to the larger population level and whether local observations are indicative of what is happening system-wide are very often unclear.

Evidence of negative effects of hypoxia on coastal fish population abundance is also not readily apparent in long-term fisheries landings data. For example, declines of demersal species in shrimp trawl bycatch in Louisiana, USA can be correlated with hypoxia; however, determining cause and effect is difficult because dynamics of the shrimp fishery are confounded with management actions and interannual variation in other factors than hypoxia (Chesney et al. 2000, Cowan et al. 2008). Broader analyses of fisheries data also supports the contention that

evidence of population-level effects are lacking. Breitburg et al. (2009b) examined fishery landings in estuaries and semi-enclosed seas worldwide and, while a negative correlation between the extent of hypoxia and average annual landings of benthic species was somewhat evident, they concluded the likelihood or severity of observed declining long-term temporal trends in demersal landings could not be directly attributed to increasing hypoxia. Clearly, though, caution is needed in interpreting landings or catch data as an index of abundance.

Analyses based on ecological and population models suggest direct effects of hypoxia on fish populations are small to moderate, leaving open the possibility of indirect effects having the potential to generate large population responses. Direct effects are reductions in growth, reproduction, or survival of individuals due to exposure to low DO, which then lead to population level changes. Indirect effects would include displacement of individuals to inferior habitat that resulted in slower growth and changes in predator behavior that led to increased or decreased mortality of the species of interest. Rose et al. (2009) describe a suite of population models and concluded that the modeling evidence suggests direct effects of hypoxia on coastal fish populations are generally small, unless exacerbated by interactions with other environmental or biological factors. Rose et al. (2009) also noted that an alternative explanation for the seemingly small population level responses predicted by the reviewed models was that certain direct effects (e.g., reproductive impairment) have historically been ignored, the high uncertainty in quantifying exposure, and the general difficulty in modeling fish population responses to variation in other environmental factors making isolating hypoxia effects difficult. Several of the models reviewed were capable of generating moderate to large population responses under certain conditions, but these conditions were considered idealized or unlikely to occur in most natural situations.

In this thesis, I present a spatially-explicit, individual-based population dynamics model of Atlantic croaker (*Micropogonias undulates*) in the northwestern Gulf of Mexico (NWGOM), and use the model to examine the effects of hypoxia on population level responses. Atlantic croaker in the NWGOM is a good case study for examining the possible population level effects of hypoxia. Atlantic croaker is a demersal, estuarine-dependent sciaenid that frequently inhabits highly productive areas along the Texas-Louisiana shelf that are susceptible to hypoxia development. This zone of hypoxia (called the "Dead Zone") has been well monitored and varies in magnitude and duration from year-to-year (Rabalais et al. 2007). The Dead Zone has also garnered a lot of scientific and public interest (National Research Council 2008), and various plans have been put forth for reducing the nutrient loadings from upstream in the Mississippi River watershed in order to reduce the degree of hypoxia in the NWGOM (Mississippi River/Gulf of Mexico Nutrient Task Force 2008). There is also a relatively large database accumulated on laboratory and field studies on how low DO affects growth, mortality, reproduction, and movement of croaker and related species. Thus, modeling of croaker in the NWGOM offers an opportunity for quantitative evaluation of the population level effects of hypoxia on a common coastal fish species.

Hypoxia and Croaker in the NWGOM

Hypoxia in the NWGOM typically appears west of the Mississippi River mouth in water depths of 5-60 m, extending as far as 55-130 km offshore, and is most severe, widespread, and persistent from June to August (Rabalais et al. 2001, 2007). Hypoxia typically occupies the lower 20-50% of the water column below the pycnocline depth (Rabalais et al. 2002). The areal extent of seasonal hypoxia in the NWGOM averaged 13,500 km^2 from 1985 to 2010, with a low value of 40 km^2 in 1988 and a maximum value of 22,000 km^2 in 2002 (www.gulfhypoxia.net).

The areal extent has exceeded the 1985-2010 long-term average in 7 of the last 10 years, suggesting a possible increasing trend in recent years. The greater incidence of hypoxia since the turn of the century may be explained by a declining threshold for hypoxia, whereby ecosystems more easily becomes hypoxic (less resistance) due to their altered biogeochemical and ecological states (Stow et al. 2005, Conley et al. 2009).

Atlantic croaker in the NWGOM spend much of their life on the Louisiana-Texas continental shelf. Spawning occurs offshore and commences in September, peaks in October, and can persist into March (White and Chittenden 1977, Sheridan et al. 1984). Eggs, yolk-sac larvae, ocean larvae are transported from off shore throughout late fall and winter (Hansen 1969, Rooker et al. 1996, Baltz and Jones 2003), and arrive in the nearshore nursery habitat and in estuaries as estuary larvae (typically 60-90 days of age) during late fall through the winter. Estuary larvae settle out in shallow marsh areas, moving into deeper inshore waters while transitioning to early juveniles. Late juveniles of intermediate size begin "bleeding off" to the shelf (i.e., offshore) in early summer; size-at-emigration increases as the summer season progresses (Yakupzack et al. 1977). Juveniles join adults offshore during the summer; gonadal development in competent YOY and recrudescence in adults likely begins in summer and early fall (Hansen 1969, White and Chittenden 1977, Sheridan et al. 1984, Thomas et al. 2007).

Croaker can be affected by the low DO associated with hypoxia via their reproduction, growth, and mortality. Exposure occurs when croaker aggregate in and around the hypoxia area during the summer months, prior to their migration to mid- and outer-shelf spawning grounds. Recent evidence has demonstrated that summer exposure to hypoxia affects fecundity during spawning in the following fall and winter (Thomas et al. 2007). Hypoxia can also affect growth and mortality of juveniles and adults. Exposure to low DO can occur for larvae and juveniles

while in estuaries (localized hypoxia rather than the Dead Zone), and due to the Dead Zone while juveniles move during the summer from the estuaries into progressively deeper waters on the shelf. Low DO has been shown to cause slowed growth (McNatt and Rice 2004) and increased mortality (Shimps et al. 2005) in laboratory experiments with spot (*Leiostomus xanthurus*). Croaker movement patterns determine their actual exposure to low DO. Croaker seem to be relatively tolerant of low DO (Eby and Crowder 2002, Craig and Crowder 2005) and thus potentially experience low enough DO concentrations to cause direct effects on reproduction, growth, and mortality.

METHODS

Description of the Model

Overview

The population dynamics of Atlantic croaker in the NWGOM were simulated by a model depicting hourly growth, mortality, reproduction, and movement of individual croaker from fertilization until age 8 years old for a period of 100 years on a 2-dimensional grid. The grid domain roughly encompassed a rectangular area from Mobile Bay, AL southwest to East Matagorda Bay, TX (28.00°N to 30.70°N and 87.60°W to 95.96°W). The model year was 365 days long beginning on September 1. Daily water temperature and food availability were specified for each spatial cell for a typical year (climatological conditions), and these conditions were repeated year after year. The environmental conditions were specified to represent near-bottom conditions because croaker is demersal. Growth was represented using a bioenergetics approach with temperature and food availability as inputs. Mortality was stage-dependent, while maturity and fecundity were size-dependent. Movement was based on both a kinesis approach with temperature as the cue and neighborhood search to allow for avoidance of low DO. Movement determined the hourly position of each individual in the grid, and thus determined the exposure of each individual to DO. Growth, mortality, and fecundity were reduced based on accumulated exposure to DO using vitality-repair sub-models (Neilan and Rose *in prep*).

Grid Configuration and Environmental Variables

The 2-dimensional grid was 300 x 800 cells, with each cell measuring 1 km^2 (Figure 1). Bottom elevation of each cell was specified by linearly interpolating elevations from 1'' bathymetry data (http://topex.ucsd.edu/marine_topo/). The coastline was specified within the grid of cells based on 2'' coastline data (http://www.ngdc.noaa.gov/mgg/shorelines/). All cells at

or below mean sea level were considered aquatic habitat (i.e., water cells). Cell elevations used the actual bottom elevation until 100 m was reached, after which, cells were assumed to be at 100 m elevation. Atlantic croaker is not typically found at depths greater than 100 m (Moore et al. 1970, Chittenden and Moore 1977). Nursery areas for the early juvenile and late juvenile stages were delineated from adult habitat by roughly following the 5 m and 10 m elevation isopleths.

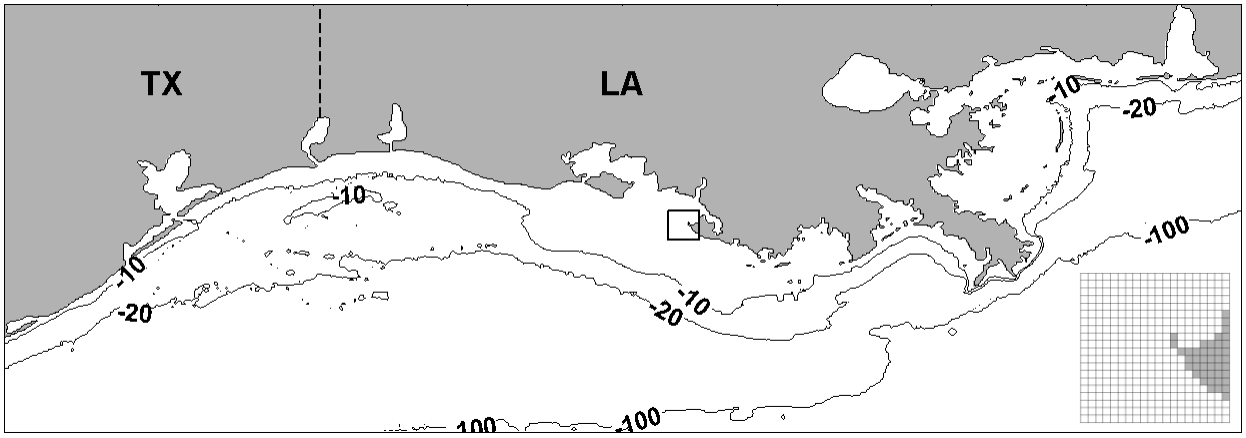

Figure 1: Model grid for the northwestern Gulf of Mexico showing cell elevation, and the Louisiana and Texas portions of the grid (denoted by dashed line). A magnified 20 x 20 cell area of the grid (outlined by the square) showing individual grid cells is displayed in the lower right corner.

Daily water temperature (°C) and chlorophyll-a (mg/m^3) values were specified for each cell on the spatial grid for each day of the year using spatial and temporal interpolation of field or satellite data. Values on the middle day of each month are shown for temperature in Figure 2 and for chlorophyll-a in Figure 3. The source for the water temperatures was 1/4° climatological mean monthly data available from the National Oceanographic Data Center. Observations were available for a climatological year for 481 locations (roughly 1 degree past the grid edges) at depths of 0, 10, 20, 30, 50, 75 and 100 meters. I used values from the surface to the elevation of each cell, but no deeper than 100 m.

The source for the chlorophyll-a concentrations, which was used as an index of prey abundance for croaker, was 0.08° climatological mean monthly values processed by the Ocean Biology Processing Group from SeaWiFS images acquired from January 1998 through December 2007. Monthly surface chlorophyll values at 5,750 points were available for an area 1° larger than the grid domain from the Goddard Earth Sciences Data and Information Services (http://disc.sci.gsfc.nasa.gov/giovanni/). Surface chlorophyll-a concentration was assumed to be a reasonable index of food availability based on others reporting empirical relationships between chlorophyll-a and fish production within a system (Ware and Thompson 2005) and across ecosystems (Ryther 1969). While daily water temperature was used directly in the croaker model, chlorophyll-a was first standardized (e.g., between 0.5 and 1) to generate multipliers for maximum consumption in the croaker bioenergetics model. Possible discrepancies between SeaWiFS observations and in situ data due to known contaminating factors associated with satellite data were assumed to be minor because SeaWiFS observations and in situ chlorophyll-a measurements are fairly well correlated in the Gulf of Mexico (Gregg and Casey 2004), and because only the temporal and spatial patterns of chlorophyll-a (not the absolute values) were important in the model.

The spatial and temporal interpolation used kriging and Fourier regression for water temperature and kriging for chlorophyll-a. Kriging was used to provide values at regular intervals (i.e., every 25 km for temperature; every 1 km for chlorophyll-a) for the entire grid for each month. For each month, this resulted in 429 kriged data values (13 x 33) for temperature and grid-wide values (300 x 800) for each month for chlorophyll-a. An additional step (Fourier regression) was needed to resolve temperature values to the level of a value for each cell on the model grid. A Fourier regression model was fit to each monthly time series of temperature

values at each of the kriged locations (i.e., 429 models). The regression models were then used to generate daily values for each kriged location, allowing temperature to be determined for the center of each grid cell each day by bi-lateral interpolation of the values at the kriged locations for that day. Daily chlorophyll-a values specified for each cell were simply updated each month.

Three hypoxia scenarios, classified by the areal extent (km^2) of hypoxia, (mild, intermediate, and severe) were simulated (Figure 4). DO values were specified daily for each spatial cell. Normoxic conditions were defined by assigning every cell a DO value of 8.0 mg/L for every day of the year. The three hypoxic conditions were represented by specifying DO values less than 8 mg/L for specific cells and time periods during the summer. DO values for each cell were determined by analysis of a map depicting the frequency of occurrence of hypoxia off the Louisiana Coast (http://www.gulfhypoxia.net). The map showed the percent frequency (<25, 25-50, 50-75, >75) of all samples for 1985-2005 that had DO < 2.0 mg/L. I used the map to derive the DO values for the grid cells under mild, intermediate, and severe scenarios (Appendix A). Average DO values within the "Deadzone" under the mild, intermediate, and severe scenarios were 4.46 mg/L, 2.23 mg/L, and 1.12 mg/L. My derived hypoxic maps on the grid were qualitatively similar to kriged maps based on field data from surveys conducted over two week periods in July for selected years (Brenda Babin, personal communication).

The hypoxic conditions were allowed to gradually set-up from normoxic conditions. I linearly interpolated DO values in each cell from the normoxic conditions on June 1 to the desired DO values on the maps over a 7 day period. Time series plots of DO at a sampling station generally in the middle of the hypoxic zone (Station C) showed that about 5-10 days were needed for DO concentrations to go from normoxia to hypoxia (Brenda Babin, personal communication).

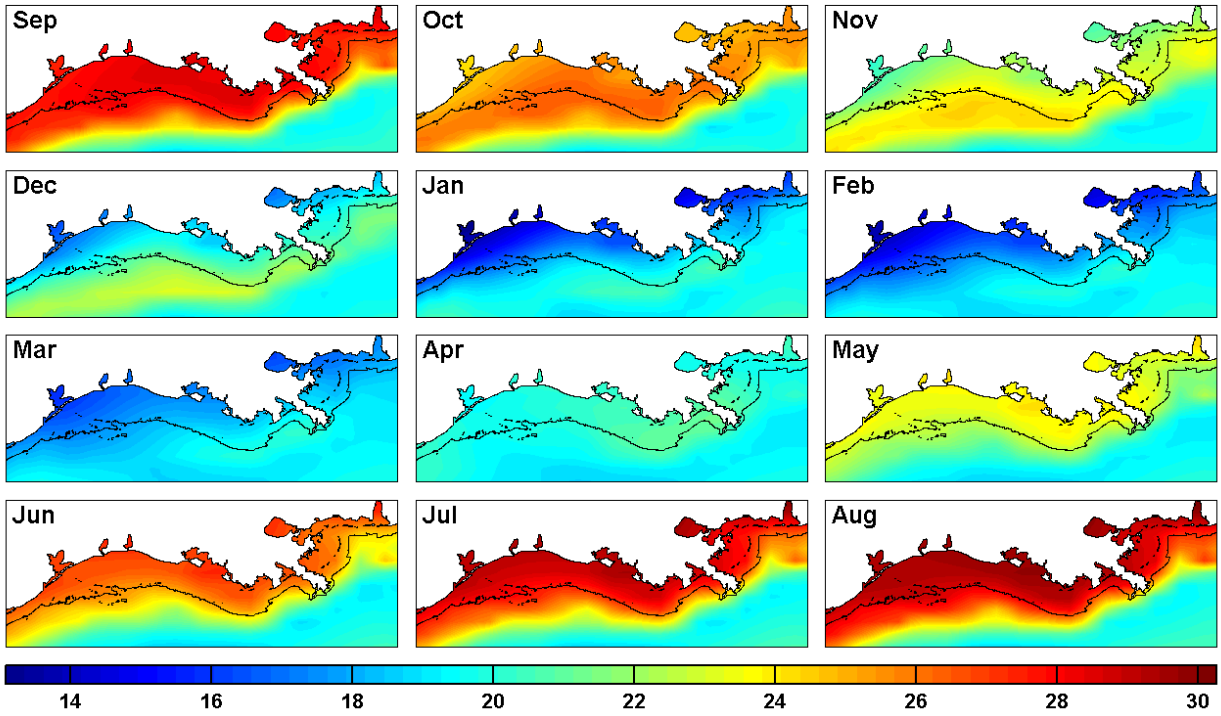

Figure 2: Snapshots of daily temperatures (°C) used in model simulations. Note snapshots show temperatures occurring on the 15th day of each month.

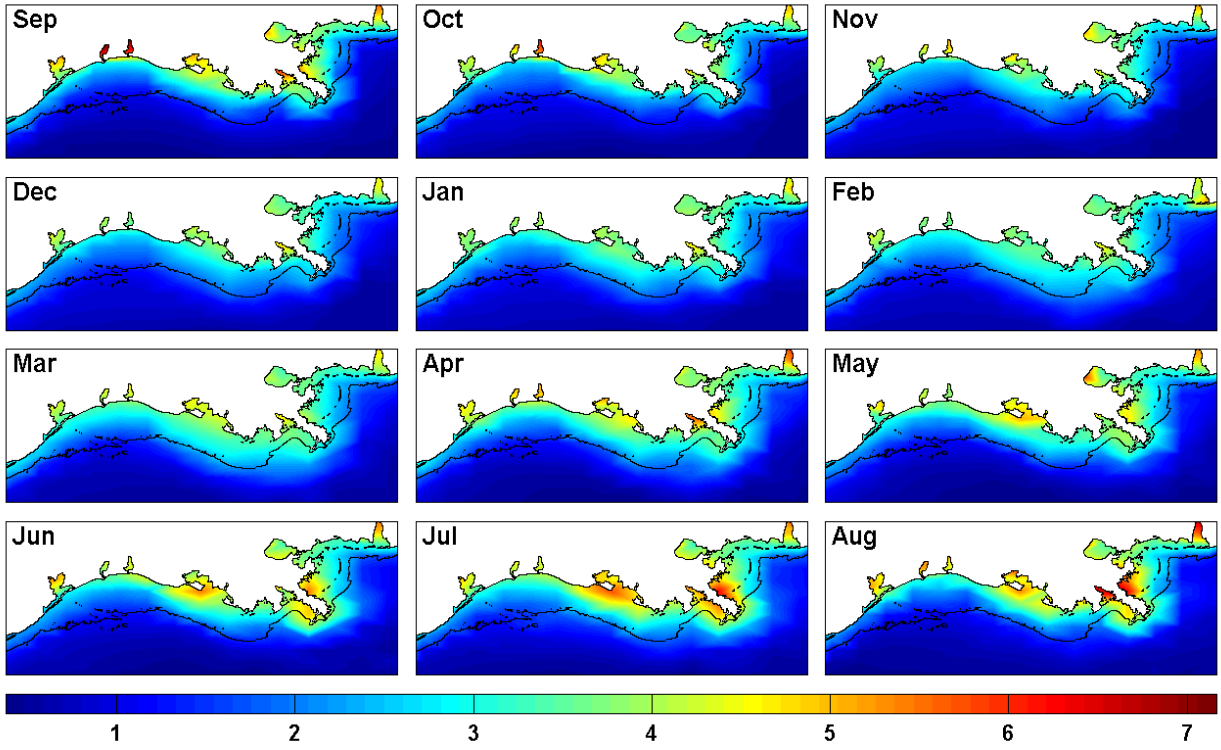

Figure 3: Snapshots of daily chlorophyll-a values (mg/m^3) used in model simulations. Note snapshots show square-transformed Chl-a values occurring on the 15th day of each month.

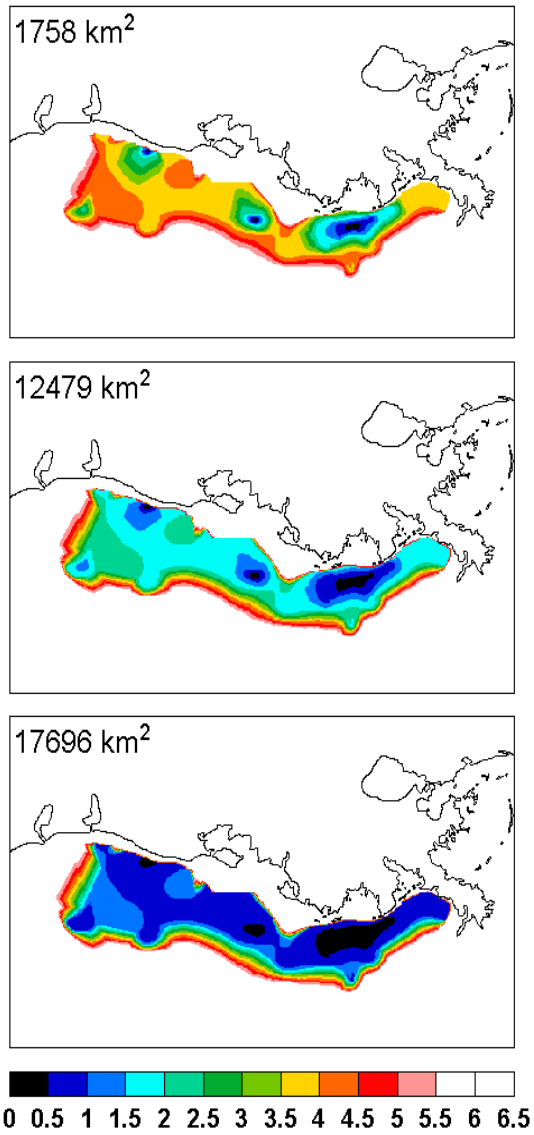

Figure 4: Maps showing the spatial distribution of DO (mg/L) for each hypoxia scenario (top = mild, middle = intermediate and bottom = severe) used in the model. Numbers in upper left-hand corner correspond to the areal extent of hypoxia (DO < 2.0 mg/L) in each scenario.

Development and Growth

Simulated croaker progress through 7 life stages (egg, yolk-sac larvae, ocean larvae, estuary larvae, early juvenile, late juvenile, and adult), and were followed as adults until they reached their eighth birthday when they were removed from the simulation. All individuals celebrated their birthday on September 1. Development through the egg, yolk-sac larva, ocean larva, and estuary larva stages was based on temperature. Transition between early juvenile and late juvenile was length-dependent (97.5 mm); late juveniles became adults when their total length exceeded 180 mm. Eggs, yolk-sac larvae, ocean larvae, and estuary larvae were followed as individuals that experienced grid-wide averaged temperatures. Upon entering the early juvenile stage, individuals were assigned a weight and length (32 mm TL and 0.28 g), and were positioned on the 2-D spatial grid, and then followed hourly as individuals through growth, mortality, reproduction, and movement. Because the transition of late juveniles to adults was length-based, there were age-1 juveniles (individuals still less than 180 mm after September 1) and there were age-0 adults (individuals that exceeded 180 mm in their first year before September 1). Development and growth were carefully calibrated so the average number of days individuals spent in the egg, yolk-sac larva, ocean larva, estuary larva, early juvenile and late juvenile stages were similar to stage duration estimates reported by Murphy (2006) (Table 1).

Egg, yolk-sac larva, ocean larva, and estuary larva development was temperature-dependent. Each hour, the stage-specific fractional development (*FD*) was computed:

$$FD = \begin{cases} 0.0957 \cdot e^{0.06931 \cdot \bar{T}}, & \text{if stage} = \text{egg} \\ 0.0610 \cdot e^{0.06931 \cdot \bar{T}}, & \text{if stage} = \text{yolk-sac larva} \\ 0.0045 \cdot e^{0.06931 \cdot \bar{T}}, & \text{if stage} = \text{ocean larva} \\ 0.0082 \cdot e^{0.04055 \cdot \bar{T}}, & \text{if stage} = \text{estuary larva} \end{cases} \quad (1)$$

The grid-wide averaged temperature on each day ($\bar{T}$) was used because these life stages were not spatially located in specific cells on the grid. A running sum of fractional developments was updated each hour and when the summed value exceeded one, development to the next life stage occurred.

Table 1: Mortality (d^{-1}) and stage duration (days) values for the egg, yolk-sac larva, ocean larva, estuary larva, early juvenile, late juvenile, and adult stages from Murphy (2006). Daily mortality rates were converted to hourly rates and used directly in the model. Stage duration estimates from Murphy (2006) were used as target values for stage durations derived from the fractional development functions and bioenergetics models.

	Model Inputs		Target Values
Stage	Mortality		Duration
Egg	0.4984		2
Yolk-sac larva	0.1645		4
Ocean larva	0.0900		45.5
	LA	TX	
Estuary larva	0.0387	0.0414	54
Early juvenile	0.0233	0.0412	73
Late juvenile	0.0185	0.0305	180
Adult	0.0012	0.0012	365

The growth of each juvenile and adult croaker was computed hourly based on local conditions in their cell and a bioenergetics model. The bioenergetics model followed the Wisconsin formulation (Hanson et al. 1997):

$$W_t = W_{t-1} + [C - (R + SDA + Eg + Ex)] \cdot W_{t-1} \cdot \frac{\rho_p}{\rho_f} \cdot \left(\frac{1}{24}\right) \qquad (2)$$

where *C* is consumption, *R* is respiration, *SDA* is specific dynamic action, *Eg* is egestion, *Ex* is excretion, and ρ_p and ρ_f are energy densities (Joules/g) of the prey and fish. The units of all rates are g prey/g fish/day. The prey-to-predator energy density ratio converted the units of weight

change from g prey/g fish/day to g fish/g fish/day. All daily rates were divided by 24 hours (equation 2) to obtain hourly rates. As a result of calibration, separate parameter sets were ultimately specified used for three size classes (< 9 g, 9-62 g, and > 62 g) (Table 2).

Table 2: Parameter values used in the bioenergetics submodel for < 9.0 g (denoted with an "a"), 9.0-62.0 g (denoted with a "b"), and > 62 g (denoted with a "c") Atlantic croaker.

Symbol	Description	Value
Consumption (C)		
ca	Intercept for Cmax	0.405[a,b,c]
cb	Slope for Cmax	0.342[a,b,c]
cq	Temperature for ck1	10.04[a,b,c]
cto	Temperature where Cmax = 0.98	29.0[a], 35.0[b,c]
ctm	Temperature ≥ cto where Cmax = 0.98	29.0[a], 35.0[b,c]
ctl	Temperature for ck4	31.00[a], 35.66[b], 35.75[c]
ck1	Proportion of Cmax at cq	0.400[a], 0.170[b], 0.115[c]
ck4	Proportion of Cmax at ctl	0.9385[a], 0.982[b,c]
Respiration (R)		
ra	Intercept for R(weight)	0.0094[a], 0.00298[b,c]
rb	Slope for R(weight)	0.000001[a], 0.102[b], 0.216[c]
rq	Rate coefficient for lower temperatures	3.1377[a], 0.0446[b], 0.0595[c]
rto	Temperature where R = Rmax	21.199[a]
rtm	Temperature where R = 0	38.613[a]
act	Increase in R due to swimming activity	1.0[a,b,c]
sda	Proportional costs of ingestion	0.172[a,b,c]
oxy	Oxycalorific coefficient	3.6770[a,b], 3.4289[c]
Egestion and Excretion		
eg	Proportion of C lost due to egestion	0.1[a,b,c]
ex	Proportion of C lost due to excretion	0.1[a,b,c]
Energy Density		
pdens	*Energy density of prey (joules g^{-1})	3687.78[a,b], 3954.565[c]
fdens	*Energy density of croaker (joules g^{-1})	5100.0[a,b,c]

*Information on diet composition and energy density of both prey and croaker were obtained from Nye (2008) and Kevin Craig (unpublished data).

Consumption depended on maximum consumption, and maximum consumption and respiration were computed based on weight and temperature. Maximum consumption (C_{max}) and respiration (R) used allometric functions ($C_{max} = ca \cdot W^{cb}$; $R = ra \cdot W^{rb}$). The temperature effect functions [$f(T)$] for C_{max} used a six parameter function (*cq, cto, ctm, ctl, ck1, ck4*), for respiration used a simple Q10 for < 9 g fish and a three parameter dome-shaped function (*rq, rto, rtm*) for 9-62 g and > 62 g fish (Appendix B). Egestion (*Eg*) was computed as a fraction (*eg*) of consumption ($Eg = eg \cdot C$); *SDA* and excretion were computed as fractions (*ex, sda*) of consumption minus egestion [$SDA = sda \cdot (C - Eg)$; $Ex = ex \cdot (C - Eg)$].

I made major modifications to Nye's (2008) bioenergetics model for croaker that was developed for the Chesapeake Bay by changing the croaker size limits that separated the three parameter sets and by adjusting consumption and respiration related parameter values. These modifications were necessary due to warmer temperatures and longer growing season in the Gulf of Mexico. I used grid-wide averaged daily temperatures and simulated the growth of a single fish from early juvenile through age-8 to determine realistic parameter values (see Calibration). One major deviation from the Wisconsin formulation of the bioenergetics model was that I made consumption (C) dependent on chlorophyll-a concentration in the cell. As is typical of Wisconsin-style models, consumption rate was computed as the product of prey availability (p-value) times a maximum consumption rate ($C = p \cdot C_{max}$). The p-value (p) represents the proportion of maximum consumption realized by an individual in its current cell. In traditional Wisconsin model applications, p-values are determined by calibration so the model predicts realistic weights at the end of a year. Instead, I used the chlorophyll-a concentration in each cell to determine the value of p each hour (Figure 5):

$$p = 0.8415 + 0.020 \cdot ln(Chl \,/\, (52.0 - Chl)^{3.83}) \qquad (3)$$

The logit-like model (equation 3) used to relate p-values to chlorophyll-a concentrations was chosen because it generated realistic growth (values of *p* between 0.55 and 0.65) across a broad range of the chlorophyll-a concentrations used as input to the model (Figure 3). Within a model year, the relative frequency of chlorophyll-a values between 1.5 mg/m^3 to 22.8 mg/m^3 was approximately 50%, with 99% of all chlorophyll-a values being less than 22.8 mg/m^3. Thus, generated p-values were typically less than 0.65, and thus on the slowly de-accelerating part of the relationship. Although rarely used, the relationship was assumed to accelerate after about 35 mg/m^3 to mimic the idea that extremely high chlorophyll-a concentrations would be associated with blooms and therefore very high zooplankton (food) levels and high feeding for croaker.

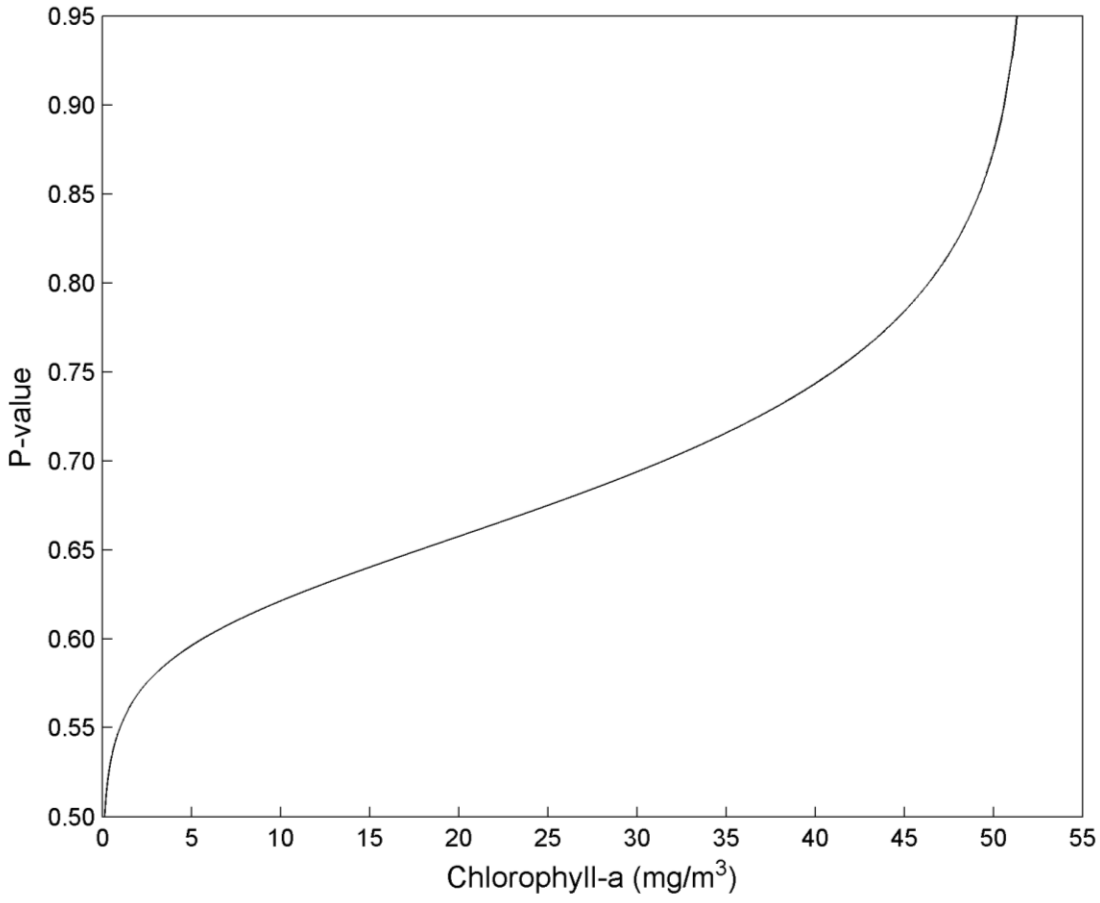

Figure 5: Relationship between chlorophyll-a and the proportion of maximum consumption (p-value).

Total length (mm) was then updated from weight (g) each hour by back calculating from the length-weight relationship reported by Barger (1985):

$$W = 5.302 \cdot 10^{-6} \cdot TL^{3.134} \quad (4)$$

Individuals could lose weight but not length; maximum weight loss per hour was constrained to ≤ 1% of current weight. Length was only updated if the individual was at the weight expected from its length.

Mortality

Three sources of mortality, in addition to hypoxia, were represented: natural (M), fishing (F), and starvation. Daily mortality rates, specified by stage and specific to Louisiana and Texas estuaries (Table 1) were obtained from Murphy (2006). For the purpose of assigning regional mortality rates, cell columns 1-200 on the model grid were considered Texas while cell columns 201-800 were considered Louisiana (Figure 1). Mortality rates for eggs and yolk-sac larvae were based on egg size and yolk-sac larvae growth rate (Murphy 2006). Mortality rates of ocean larvae, estuary larvae, early juveniles were estimated by Murphy (2006) from growth rate-based relationships or from catch-curve analyses of Louisiana and Texas long-term field data. Annual mortality rates (F + M) specified for late juveniles were based on the Draft Fishery Management Plan for Groundfish (GMFMC 1980). The natural mortality rate for adult croaker (0.37 yr^{-1}) in the Gulf of Mexico was derived from growth parameters and average occupied water temperature, and combined with an assumed fishing mortality rate of 0.07 yr^{-1} to account for mortality due to incidental bycatch by the shrimp fishery, to obtain a total rate of 0.45yr^{-1}. All mortality rates were converted to hourly rates for use in the model.

Starvation mortality was based upon an individual's weight relative to its threshold weight. Juvenile and adult croaker lost weight if metabolic demands exceeded consumption.

Threshold weight for starvation was considered to be 50% of the expected weight based on individual's current length. When an individual starved, it was removed from the simulation.

Late juvenile was the only stage assumed to have density-dependent mortality. Compensatory density-dependent processes operate to slow population growth at high densities and increase population growth at low densities (Rose et al. 2001). The juvenile stage in many fishes is commonly thought to be a life stage where density-dependent growth and mortality commonly occurs (Myers and Cadigan 1993, Cowan et al. 2000, Houde 2008). Using long term sampling of young-of-the-year croaker in Texas and Louisiana estuaries, Murphy (2006) showed a positive relationship between apparent loss rates (slope of log-transformed catch versus time) and average abundance of late juvenile croaker. I used a similar relationship in this model. A multiplier based on the standardized abundance of late juveniles in a cell was used to adjust the constant total late juvenile mortality rate each hour (Figure 6). Each hour, abundance of late juveniles in each cell is divided by a specified abundance to obtain the standardized abundance, and then the multiplier was determined from Figure 6 and applied to the mortality rate for that hour. The specified abundance used to standardize late juvenile abundance was determined during calibration.

Reproduction

On September 1 of each year, all individuals were evaluated for maturity based on their length. Probability of being mature increased with total length (*TL*):

$$P(mature) = 1/(1 + 1.572 \cdot 10^{8} \cdot e^{-0.1156 \cdot TL}) \quad (5)$$

For each individual, if a randomly generated value between 0 and 1 was less than *P(mature)*, then that individual was deemed mature. All mature individuals on September 1 were then assigned a degree-days value from a triangular probability distribution with minimum, mode, and

maximum values (20, 200, and 450). Maturity and the assigned degree-days value were kept by individuals for the remainder of their life. Every individual spawned eggs, but their egg production was multiplied by 0.5 to account for a 1:1 male to female ratio.

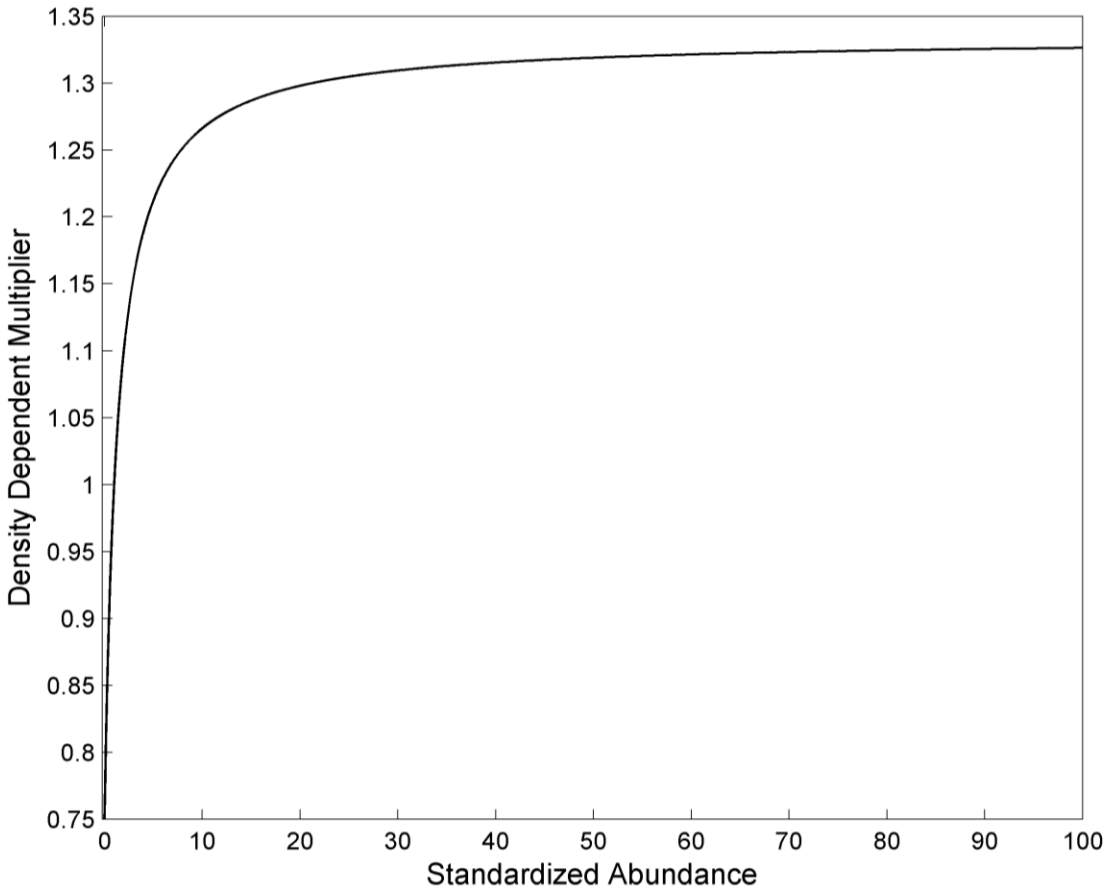

Figure 6: Relationship between standardized abundance (Σ $worth_{cell(i, j)}$ / 1760 km^{-2}) and mortality. Density-dependent mortality was imposed on individuals in the late juvenile stage.

Day of spawning for each individual was determined by degree-days. Degree-days were computed each day for each mature individual by summing the difference between the temperature in the occupied cell and a specified temperature threshold (17°C) below which degree days were not increased. When an individual accumulated its assigned degree-days value, they initiated spawning on that day. Each individual was able to release up to 12 batches; one every 3 days over a consecutive 34 day period. Eggs per batch for each of the 12 batches

was derived from a relationship between weight (g) and potential annual fecundity reported by Sheridan et al. (1984):

$$F = -3248 + 1179 \cdot W \quad (6)$$

Each batch consisted of $F/12$ eggs; annual fecundity was re-computed using the weight on the each day of batch release during the 34 days. The total actual annual number of eggs spawned by each individual was the sum of eggs spawned over all its batches.

Movement

Hourly movement was modeled using a kinesis algorithm that simulated the behavioral swimming response of croaker to local conditions. The position of each juvenile and adult individual was tracked in x-y continuous space (i.e., x-y distance in meters from the lower left corner of the grid) and in discrete grid space (i.e., cell number). Kinesis is an approach to modeling movement in which organisms respond to external cues by changing their velocity and turning frequency (Benhamou and Bovet 1989; Humston et al. 2004). The velocity of the individual in each of the x and y directions was the sum of two components: inertia from the velocity in the previous hour [$f(v_{t-1})$, m/hour] and a randomly generated velocity [$g(\varepsilon)$, m/hour]:

$$\begin{aligned} x_{t+1} &= x_t + f(v_{t-1}) \cdot \Delta t + g(\varepsilon) \cdot \Delta t \\ y_{t+1} &= y_t + f(v_{t-1}) \cdot \Delta t + g(\varepsilon) \cdot \Delta t \end{aligned} \quad (7)$$

where Δt is the time step (i.e., one hour). A weighting function that depended on how close water temperature was to a pre-defined optimal value was used to determine the relative contribution of inertial versus random velocities:

$$\begin{aligned} f(v_{t-1}) &= v_{t-1} \cdot h_1 \left[e^{(-0.5)\left[(T - T_{opt})/\sigma_T\right]^2} \right] \\ g(\varepsilon) &= \varepsilon \cdot \left[1 - h_2 \left(e^{(-0.5)\left[(T - T_{opt})/\sigma_T\right]^2} \right) \right] \end{aligned} \quad (8)$$

where T is water temperature in the cell, T_{opt} is the specific optimal temperature, and ε is a random deviate from a normal distribution with mean equal to maximum sustained swimming speed ($\Phi = 3$ BL/s) and SD equal to $\Phi/2$. Maximum sustained swimming speed was converted to km per hour (i.e., $\Phi \cdot 10^{-6}$ km $\cdot$ 3600 s $\cdot$ Δt). Randomly generated velocities had an equal probability of being positive or negative. The inertial component dominates as temperature approaches the optimal temperature (T_{opt}), while movement becomes more random under sub-optimal conditions. The sensitivity and tolerance of an individual to conditions were dictated by the Gaussian height (h_1 and h_2) and variance (σ_T) parameters of the weighting scheme. Once an individual's new continuous x and y locations were determined, the individual's cell location was then updated. Movement parameters were set to generally used values (Humston et al. 2004), except for optimal temperature that is site-specific. Optimal temperature and variance parameters (σ_T) were specified the same for early juveniles, late juveniles, and adults, but values were specific to certain time periods and were determined by calibration.

Avoidance movement of low DO was simulated using a threshold value and a neighborhood search. Individuals that entered a cell with a DO value less than 2.0 mg/L initiated avoidance behavior immediately (i.e., they moved again before any exposure occurred). I decided to use a threshold value of 2.0 mg/L to trigger avoidance behavior because evidence indicates Atlantic croaker in the NWGOM avoid DO concentrations of 1.2-2.7 mg/L (Kevin Craig, personal communication). In the hour avoidance was triggered, individuals evaluated DO levels and temperatures in a 9 x 9 cell neighborhood (80 cells) centered on their current cell. They moved to the center of the cell that had DO > 2.0 mg/L and whose temperature was closest to their T_{opt}. If DO was less than 2.0 mg/L in all 80 cells, individuals moved to the cell with the highest DO, regardless of temperature.

The maximum distance an individual was able to move in a time step (1 hour) during avoidance was 6.4 km, which would require a fast swimming speed. Movement of 6.4 km required a swimming speed of ~ 9 BL/s (1780 mm/s for a 200 mm individual) for one hour. However, the effective distance for avoidance of hypoxia in test trials with the severe hypoxia scenario using the 80-cell search was about 3.6 km (median distance moved in one hour when avoidance movement was triggered); which requires a maximum sustained swimming speed of about 5 BL/s (1000 mm/s for a 200 mm individual) for one hour. Videler and Wardle (1991) reported an average maximum sustained swimming speeds (sustained for 200 minutes) of 3-4 BL/s for a variety of species; prolonged swimming speeds (< 200 minutes) are generally faster. Thus, the average of 5 BL/s during avoidance in the model simulations is fast but possible for the 60 minutes required in the model simulations. Reducing the size of the neighborhood search area (e.g. 24 cells) limits the utility of the modeled avoidance behavior and overestimates exposure because the maximum distance moved in the four cardinal directions is limited by the size of the neighborhood search area.

Exposure and Effects of Hypoxia

DO affected growth, mortality, and reproduction. Individuals were exposed to time-varying DO values as DO concentrations in cells changed and as an individual moved from cell to cell that had different DO values. Three exposure-effects submodels were used that related reduced growth, increased mortality, and reduced annual fecundity to varying exposure to DO concentrations (Neilan and Rose, in prep.). Each hour, the growth, reproduction, and survival vitality (Vg, Vr, and Vs) of an individual was computed using the same general formulation:

$$Vg, Vr, or\ Vs = \begin{cases} 1.0 - \alpha \dfrac{(DO - DO_{NE})^2}{(DO - DO_{NE})^2 + \beta^2} & \text{if DO} < \text{DO}_{\text{NE}} \\ 1.0 & \text{if DO} \geq \text{DO}_{\text{NE}} \end{cases} \qquad (9)$$

where *DO* is the DO concentration in its cell and DO_{NE} is the DO threshold below which vitality is impaired, and α and β are non-negative constants. Growth vitality also included a "repair" rate; Vg was increased by 0.169 in any hour that DO in the current hour was still below the threshold value but greater than the DO of the previous hour. Data from laboratory experiments with croaker were used to estimate vitality-repair parameters for reproduction and mortality; growth parameters were based on spot (*Leiostomus xanthurus*). The parameter values for Vg, Vr, and Vs are shown in Table 3.

Table 3: Parameter values used in the vitality-repair sub-models (Neilan and Rose *in prep*).

Parameter	Growth (Vg)	Reproduction (Vr)	Survival (Vs)
DO_{NE}	3.0	4.0	1.25
α	10.0	1.03	1.66
β	5.79	1.4	0.54

The values of vitality (0 to 1) were used as multipliers on growth, mortality, and fecundity. Growth was multiplied by Vg each hour only if growth in that hour was positive. The growth vitality-repair parameters were based on laboratory experiments with *ad lib* feeding so no weight loss occurred (Neilan and Rose *in prep*). Mortality rate was multiplied by Vs every hour. Batch size was modified based on an individual's vitality value (Vr) at the end of the hypoxia period during the previous summer. Reproductive vitality was only affected by the last 10 weeks of an individual's exposure history. Thus, the value of Vr was expressed as a simple average:

$$Vr = \frac{1}{k}\sum_{i=1}^{k} Vr(i) \qquad (10)$$

where k equals the number of time steps (1680) occurring in the final 10 weeks of the hypoxic period (June 23 to August 31).

The effects of low DO on vitality were only imposed on late juveniles, age-1 adults, and age-2 adults. Early juveniles were restricted to the nearshore habitat (< 5 m depth) and thus not vulnerable to exposure, late juveniles were restricted to less than 20 m depth and thus could be exposed. Age-3 and older adults are thought to be farther offshore and only minimally exposed.

Numerics

I used the super-individual approach (Scheffer et al. 1995) to ensure reasonable memory usage and computational times. With the super-individual approach, a fixed number of super-individuals are followed for each age-class. Each super-individual is assigned an initial worth, which is the number of identical population individuals it represents. Mortality then operates to reduce an individual's worth over time. The same number of super-individuals remains in the model throughout; when super-individuals reach their maximum age they are removed and the array spot made available to house a newly recruiting individual. All computations and output variables related to population level abundance and biomass use an individual's attributes, multiplied by its worth. The simpler approach of adding a new model individual for each new individual entering the population (i.e., initial worth is one), and eliminating individuals when they die, is not practical because millions would need to be followed and there is the possibility of exceeding array space under increasing population conditions.

Simulations used 20,000 super-individuals for each of the eight age-classes. When an individual reached its eighth birthday, it was removed from the model and its array location was made available for a new incoming individual. Each year, 20,000 super-individuals were removed and 20,000 new super-individuals were created. Each day during the spawning season, eggs were pooled together over all spawning individuals. These eggs were represented by the number of super-individuals allocated to that day; the initial worth of each the newly entering

super-individuals was computed as total eggs on the day divided by the total number of super-individuals allocated to the day. For example, a day with 2000 eggs and 10 super-individuals allocated would have each of the 10 super-individuals assigned an initial worth of 200.

Allocation of super-individuals to days within each year was based on projected spawning. Ideally, all super-individuals in a given year would start with the same initial values of worth to minimize the effects of a few super-individuals with very high worths distorting the results. I use projected spawning to try to balance the initial worths. On September 1, spawning was simulated for the upcoming year using the grid-wide averaged daily temperature and the current worths and weights of spawners (i.e., no mortality or growth over the spawning season was assumed). Each individual initiated spawning according to its assigned degree-days and spawned 12 equal batches every 3 days. Super-individuals were initially allocated in proportion to the percent of total egg production projected to occur on each day. Because integer numbers of super-individuals must be allocated, I used the nearest integer less than or equal to the allocated real number (e.g., 2.7 becomes 2). On the day after actual spawning ends, I accumulated the super-individuals not allocated (due to integer truncation) and super-individuals allocated to days when no eggs were produced. I then assigned these unused super-individuals to existing super-individuals one at a time, each time going to the super-individual with the highest value of worth as of the day after spawning. This can include super-individuals that are eggs, larvae, or juveniles. The worth of the highest-worth super-individual was then halved, and the newly introduced super-individual was given half of the worth and all of the traits of the highest-worth individual. This was repeated for each unallocated super-individual until all were entered into the model. This way, exactly 20,000 new individuals were introduced every year and super-individuals with extremely high worths were avoided.

Initial Conditions

All model simulations began with 20,000 super-individuals per age class. All individuals within an age-class were assigned a weight and length based on length-at-age data (see Figure 12), and were randomly placed on the grid. The beginning worth of each super-individual was set to a worth specific to its age-class, which was based on a specified total worths of entering age-1 (1.5 million) that was then decreased with older ages based on the adult mortality rate. Preliminary simulations provided information used to specify realistic initial conditions. However, the first twenty years of all simulations were still ignored to minimize any remaining effects of arbitrary initial conditions.

Design of Simulations

Calibration

The developmental rates of early life stages, bioenergetics model parameters, and optimal temperatures and σ_T values for movement were adjusted until averaged stage durations, length-at-age, and movement patterns agreed with reported information. The mortality rate and normalizing abundance of late juveniles were then adjusted to generate a stable population size of about 1.5×10^6 entering age-1individuals. This ensured the model adequately simulated the life history of Atlantic croaker in the NWGOM and provided an adequate baseline for later comparisons. Because I simulated an arbitrary population size, all comparisons of hypoxia effects were relative to the baseline (normoxic) simulation.

The steps in calibration were as follows. First, I adjusted development rate functions using grid-wide averaged daily temperatures until realistic stage durations of egg, yolk-sac larva, ocean larva, and estuary larva stage were obtained. Second, bioenergetics parameters were adjusted using the averaged daily temperatures until stage durations of early and late juveniles

and mean length-at-age (and associated mean weight-at-age) were reasonable. Third, optimal temperatures and σ_T values for movement were calibrated by following 1000 super-individuals in 8 years runs using the full model (i.e., 2-D grid) but without growth and mortality. Fourth, the full model was run with all of the calibrated parameter values for 100 years, and final adjustments were made to ensure the criteria met with off-grid calibration were still met in the full model. Finally, the normalizing abundance for density-dependent mortality of late juveniles was determined so a stable population of 1.5 million age-1 individuals was obtained.

In step 1, key aspects (durations, entering lengths) of life stages were calibrated to follow the typical life cycle of Atlantic croaker in the NWGOM. I assumed a typical individual was spawned during the peak spawning period (October), was 180 mm after 365 days later, and reached nearly 400 mm by the beginning of their seventh birthday. Simple exponential functions relating daily, grid-wide average water temperature and developmental rates were developed so that predicted egg, yolk-sac larva, ocean larva, and estuary larva stage durations were close to values reported by Murphy (2006). The stage durations also had to enable individuals spawned in October to transition to the early juvenile stage by February of the following year, when early juveniles are most abundant within the nursery areas (Arnoldi et al. 1973, Yakupzack et al. 1977).

In step 2, preliminary parameter values for the bioenergetics model for juveniles and adults were initially determined off-grid using daily, grid-wide average water temperatures and p-values of 0.6 to 0.65. Stage duration for the early and late juveniles was length-dependent in the model. Thus, the bioenergetics parameters were adjusted until total length, based on predicted weight, was about 97 mm (beginning TL of late juveniles) in April and 180 mm (beginning TL of adults) by the following October. Growth for a typical adult (ages 1-8) was

calibrated in the off-grid version by adjusting bioenergetics parameters so mean length-at-age agreed with values reported by Diamond et al. (1999). Optimal growth occurred at about 30°C for juveniles and cooler temperatures for older fish.

Step 3 of the calibration focused on movement and involved adjustment of optimal temperatures and σ_T values in equation (8) until movement patterns of individuals in the full grid mimicked the immigration of YOY from inshore areas to the shelf (Yakupzack et al. 1977) and the seasonal inshore-offshore migration of older ages (Moore et al. 1970). I used separate parameter values for different times of the year (Table 4) because of seasonal changes in temperature.

Table 4: Description and values of parameters used in the kinesis movement model.

Symbol	Description	Value
Φ	maximum sustained swimming speed (body lengths s^{-1})	3.0
h1	height of Gaussian curve for inertial velocity	0.98
h2	height of Gaussian curve for random velocity	0.99
σ_T	width of Gaussian curves (°C)	$3^{a,c}$, $4^{b,d}$
T_{opt}	optimal temperature (°C)	$26^{a,c}$, 29^{b}, 21^{d}

[a] Apr 16th – Jun 15th
[b] Jun 16th – Sep 15th
[c] Sep 16th – Dec 16th
[d] Dec 17th – Apr 15th

In step 4, the calibrated development and growth were re-evaluated using the full model to ensure realistic dynamics were still produced under conditions of much greater spatial and temporal variability. Variability was higher in the full model due to both the time of year individuals were spawned (temporal) and movement on the grid (spatial).

Finally, the standardized abundance for late juvenile density-dependent mortality was adjusted to obtain a stable baseline population. A standardized abundance of 1760 km^{-2} resulted in a stable population with an average age-2 and older abundance of about 1 million individuals.

Results of model calibration are shown for the final, full model simulation only. The outputs consisted of: mean stage durations, monthly spatial distributions by life stage, mean length-at-age, and mean age-2 and older abundance over time. Stage durations and length-at-age were computed by averaging values for years 61 to 100. Spatial distributions were snapshots of abundance on the grid on the 15th day of each month and were from the same year-class (year 93 for juveniles, year 94 for age-1, and year 95 for age-2). I aggregated grid cells into coarser cells so patterns were more easily seen on the spatial maps. Total worth was computed by grid cell and then summed for a new plotting grid where one cell represented a 10 x 10 cell area on the model grid. Age-2 and older abundance was computed on August 31 of each year, and thus included fish who had already had 2 or more birthdays.

Hypoxia Effects

Four simulations of hypoxic conditions were performed using the calibrated model. Three simulations were mild, intermediate, and severe hypoxia repeated every year. The fourth simulation was randomly generated time series of mild, intermediate, and severe hypoxia years. In the time series condition, there was a 0.12, 0.4, and 0.48 probability of each year being mild, intermediate, or severe. The probability of the severity of hypoxia was estimated by classifying each year (1985-2010) based on the reported areal mid-summer extent of hypoxia (http://www.gulfhypoxia.net) as either mild ($\leq$ 7000 km^2), intermediate (7001 − 15000 km^2), or severe (15001 − 22000 km^2). All simulations were for 100 years; baseline conditions for the first 20 years, followed by hypoxic conditions imposed beginning in year 21. A 20-year baseline

spin-up minimizes the effects of initial conditions on population responses to hypoxia. Twelve replicate simulations of the time series condition were performed using different random sequences of mild, intermediate, and severe years for years 21 to 100 (Figure 19). For the mild, intermediate, and severe simulations, and for each replicate time series simulation, annual abundance of age-2 and older individuals were plotted over time. Results were further summarized by computing the average abundance for years 61 to 100 of each simulation, and expressing the average as a percent of the year 61-100 average abundance in baseline.

I also examined aspects of the severe hypoxia simulation in more detail. Spatial distributions of age-2 individuals for June, July, and August in the severe simulation was shown to illustrate the avoidance movement. Exposure in the severe simulation was summarized by reporting the average percent of surviving age-1 and age-2 individuals on September 1 that experienced at least one hour of DO < 4.0 mg/L the proceeding summer and by plotting hourly mean exposure and hourly mean Vs, Vg, and Vr values of all exposed individuals on that hour. Average daily mortality over years 61-100 for age-0, age-1, and age-2 individuals were reported to show the effects of hypoxia on survival. Effects of hypoxia on growth and reproduction were shown by reporting mean weight-at-age, mean fraction of age-1 mature, and mean eggs per gram and eggs per individual, averaged for years 61-100 for the severe hypoxia simulation.

Sensitivity Analysis

A sensitivity analysis was performed using replicate 6 of the time series simulations to explore the aspects of avoidance, the relative contributions of growth, mortality, and reproduction to the overall population response, and the effects of all ages being exposed and mixing events (Table 5). Avoidance was explored by using DO values that trigger the avoidance response of 1.5 and 2.5 (compared to 2.0), and reducing the number of cells searched in the

neighborhood from 80 to 24. The contributions of growth, mortality, and reproduction were explored by performing the time series simulation with all combinations of each and pairs of the three vitality-repair submodels set to one to eliminate their effects. I also performed a simulation that allowed all ages to be exposed. The same vitality-repair submodels used for late juveniles, age-1 and age-2 in baseline were used for age-3 and older individuals. Finally, the time series simulation was repeated with random mixing events imposed in June, July, and August. Probability of one, two, and three mixing events in each month were estimated from an analysis of mixing events of time series DO data at Station C of the gulf-wide surveys for years 1989-2008 (Brenda Babin, unpublished data).

For the sensitivity analysis, baseline abundance was recomputed using the same random number seed that was used in replicate 6 of the time series simulations. The results of the sensitivity analysis was summarized by calculating the average age-2 and older annual abundance for years 61-100 of each sensitivity run, divided by the average from the replicate 6 baseline simulation.

Table 5: Summary of sensitivity runs. The sequence of hypoxia scenarios in all sensitivity runs was identical to time series replicate 6. Note that in the mild, moderate, and severe hypoxia simulations and in the time series simulations individuals avoided DO < 2.0 mg/L by searching 80 surroundings cells for either the highest DO or where DO was > 2.0 mg/L and temperature was closest to T_{opt}, only juveniles, age-1, and age-2 individuals were directly affected by low DO, and no mixing occurred.

Run	Factor Examined	Details
A	Avoidance behavior triggered at lower DO	If DO < 1.5 mg/L, individuals search 80 surrounding cells and go to the highest DO cell or the cell with DO ≥ 1.5 mg/L that has the temperature closest to T_{opt}.
B	Avoidance behavior triggered at higher DO	If DO < 2.5 mg/L, individuals search 80 surrounding cells and go to the highest DO cell or the cell with DO ≥ 2.5 mg/L that has the temperature closest to T_{opt}.
C	Avoidance behavior triggered at lower DO and searched smaller neighborhood	If DO < 1.5 mg/L, individuals search 24 surrounding cells and go to the highest DO cell or the cell with DO ≥ 1.5 mg/L that has the temperature closest to T_{opt}.
D	Searched smaller neighborhood	If DO < 2.0 mg/L, individuals search 24 surrounding cells and go to the highest DO cell or the cell with DO ≥ 2.0 mg/L that has the temperature closest to T_{opt}.
E	Avoidance behavior triggered at higher value and searched smaller neighborhood	If DO < 2.5 mg/L, individuals search 24 surrounding cells and go to the highest DO cell or the cell with DO ≥ 2.5 mg/L that has the temperature closest to T_{opt}.
F	DO effects on mortality	Vg and Vr set to one (equation 9)
G	DO effects on growth	Vr and Vs set to one (equation 9)
H	DO effects on reproduction	Vg and Vs set to one (equation 9)
I	DO effects on growth and reproduction	Vs set to one (equation 9)
J	DO effects on growth and mortality	Vr set to one (equation 9)
K	DO effects on reproduction and survival	Vg set to one (equation 9)
L	All ages are exposed to DO conditions	DO effects were imposed on all individuals based on their movement and exposure.
M	Effects of mixing events	Number of events per month and start day of each event is randomly selected. Probabilities of 1, 2, and 3 events were: 10%, 10%, and 0% for June; 10%, 5%, and 5% for July; and 20%, 10%, and10% for August. Hypoxic conditions as dictated by the mild, moderate, or severe conditions are then linearly approached so it takes 4 days from the event day to return to the appropriate DO value in each cell
N	Temperature preference excluded from neighborhood search	If DO < 2.0 mg/L, individuals search 80 surrounding cells and go to the highest DO cell.

RESULTS

Calibration

Simulated movement roughly reproduced the purported inshore-offshore seasonal migration patterns of Atlantic croaker in the Gulf of Mexico. Figures 7-11 follows individuals in the full baseline simulation that were born in year 93 for years 93-95 as they went from early juveniles through age-2. The majority of early juveniles first appeared on the grid in February (Figure 7). Starting around April 1, late juveniles were increasingly abundant across inner parts of the Texas-Louisiana shelf (Figure 8). Nearly all remaining late juveniles (those still less than 180 mm) and age-1 adults moved onto the shelf by October 1 (Figures 9-10). The majority of age-1 individuals had moved to the mid and outer regions of the shelf where spawning occurred by November, and were generally dispersed across the entire grid in May before aggregating in inshore areas in the summer (Figure 10). This seasonal inshore-offshore migration pattern was repeated the following year when these age-1 survivors become age-2 individuals (Figure 11). All adult age-classes repeated the same pattern, and the pattern was repeated in every year.

Averaged stage durations and length-at-age in the baseline simulation were comparable to reported estimates in the literature. Average stage duration in the baseline simulation was 2 days for eggs, 3 days for yolk-sac larvae, 45 days for ocean larvae, 54 days for estuary larvae, 73 days for early juveniles, and 180 days for late juveniles, similar to values reported by Murphy (2006) (Table 1). The calibration of the bioenergetics submodel showed optimal growth at 30°C for < 9g individuals, 28-30°C for 9-62.5g individuals, and 25-27°C for individuals > 62.5g. In the full baseline model simulation, the bioenergetics (equation 2) with the chlorophyll-a adjustment to consumption (Figure 5) resulted in age 1-8 mean beginning lengths very similar to reported lengths-at-age of croaker (Figure 12).

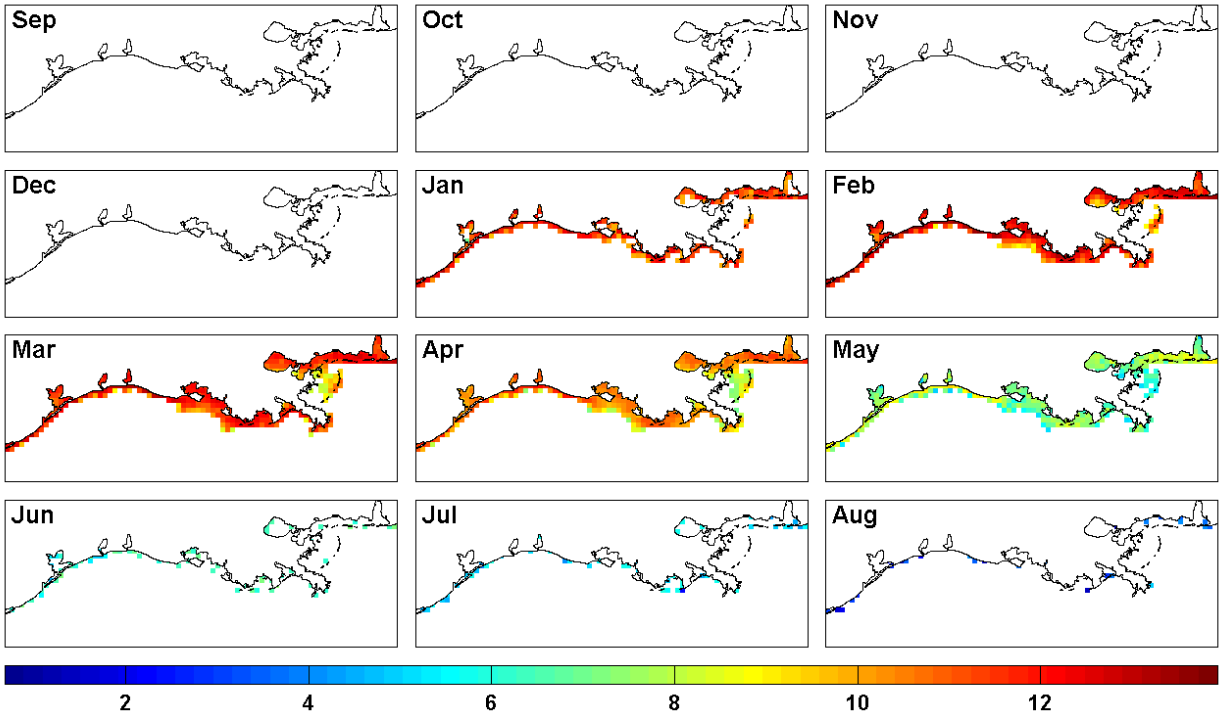

Figure 7: Mid-monthly snapshots showing the spatial distribution of early juveniles in model year 93 from baseline run. Colored pixels represent the ln-transformed number of early juveniles in a 10 x 10 cell area on the grid. Note figures 7-11 all show the same cohort.

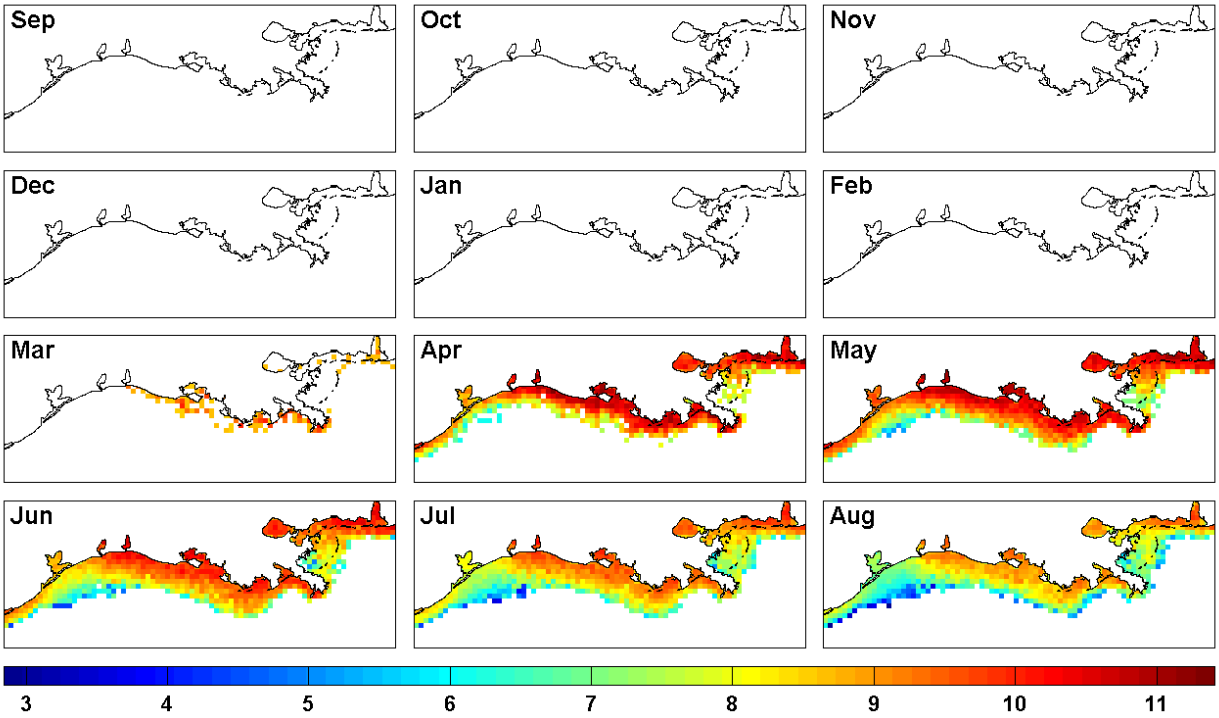

Figure 8: Mid-monthly snapshots showing the spatial distribution of age-0 late juveniles in model year 93 from baseline run. Colored pixels represent the ln-transformed number of late juveniles in a 10 x 10 cell area on the grid. Note figures 7-11 all show the same cohort.

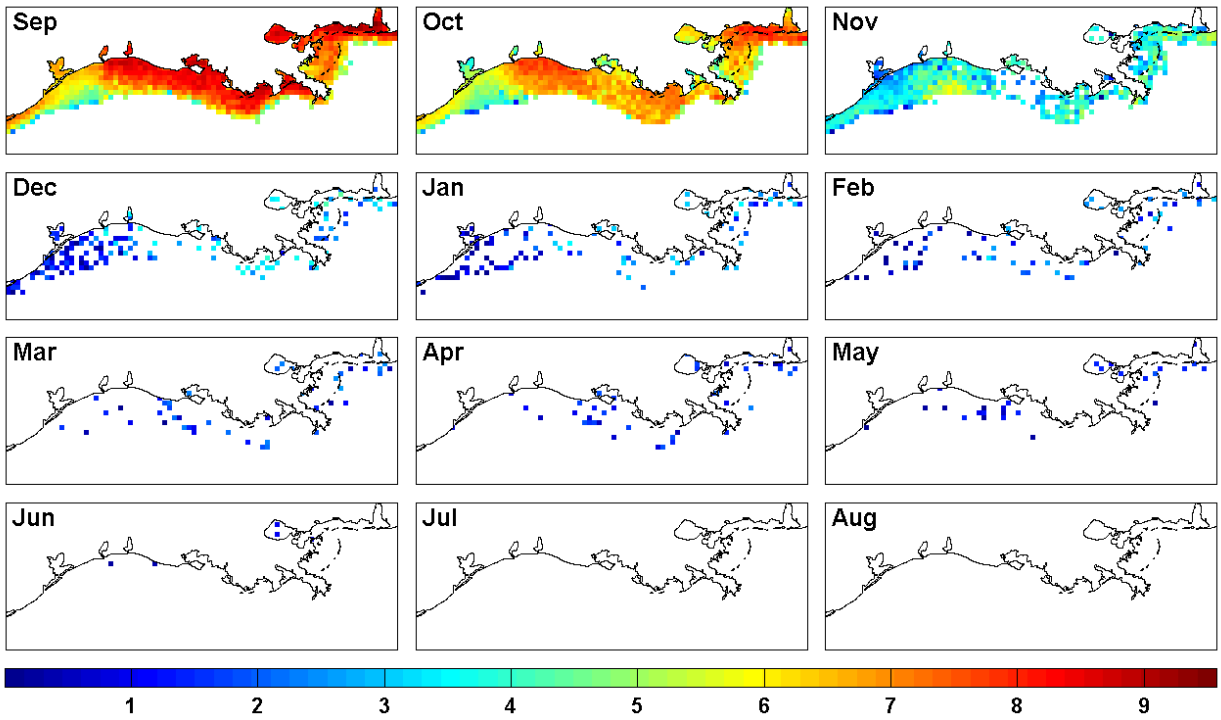

Figure 9: Mid-monthly snapshots showing the spatial distribution of age-1 late juveniles in model year 94 from baseline run. Colored pixels represent the ln-transformed number of age-1 late juveniles in a 10 x 10 cell area on the grid. Note figures 7-11 all show the same cohort.

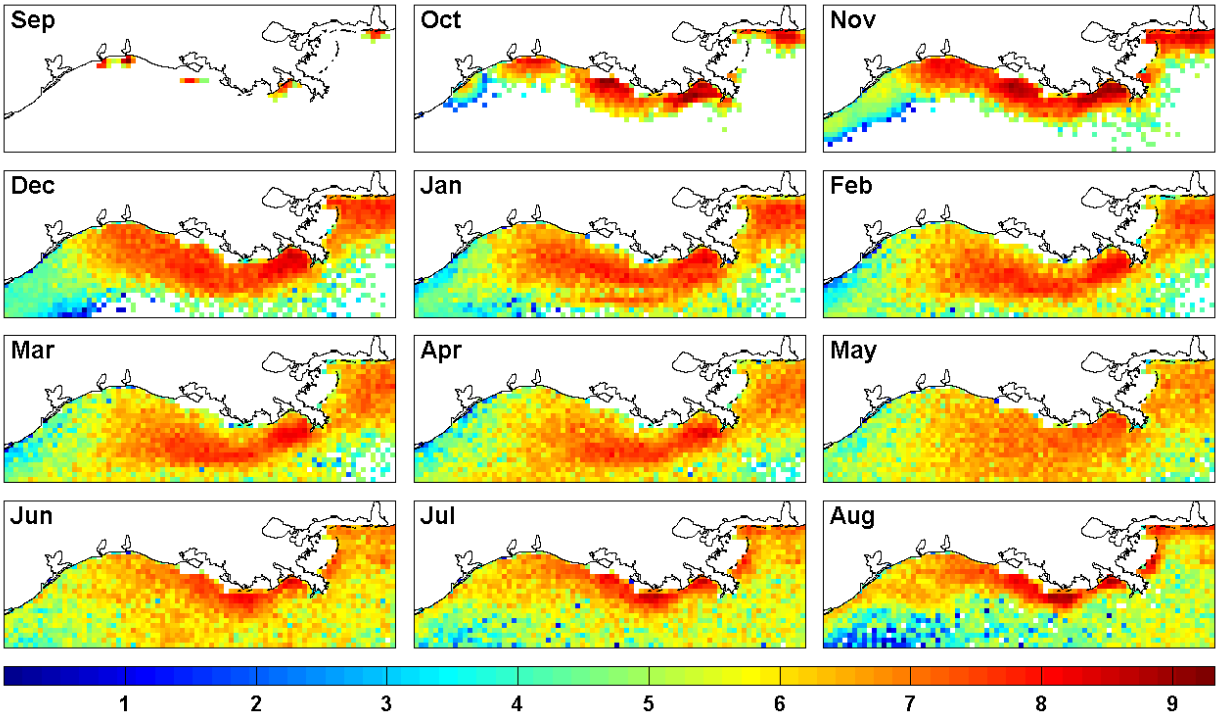

Figure 10: Mid-monthly snapshots showing the spatial distribution of age-1 adults in model year 95 from baseline run. Colored pixels represent the ln-transformed number of age-1 adults in a 10 x 10 cell area on the grid. Note figures 7-11 all show the same cohort.

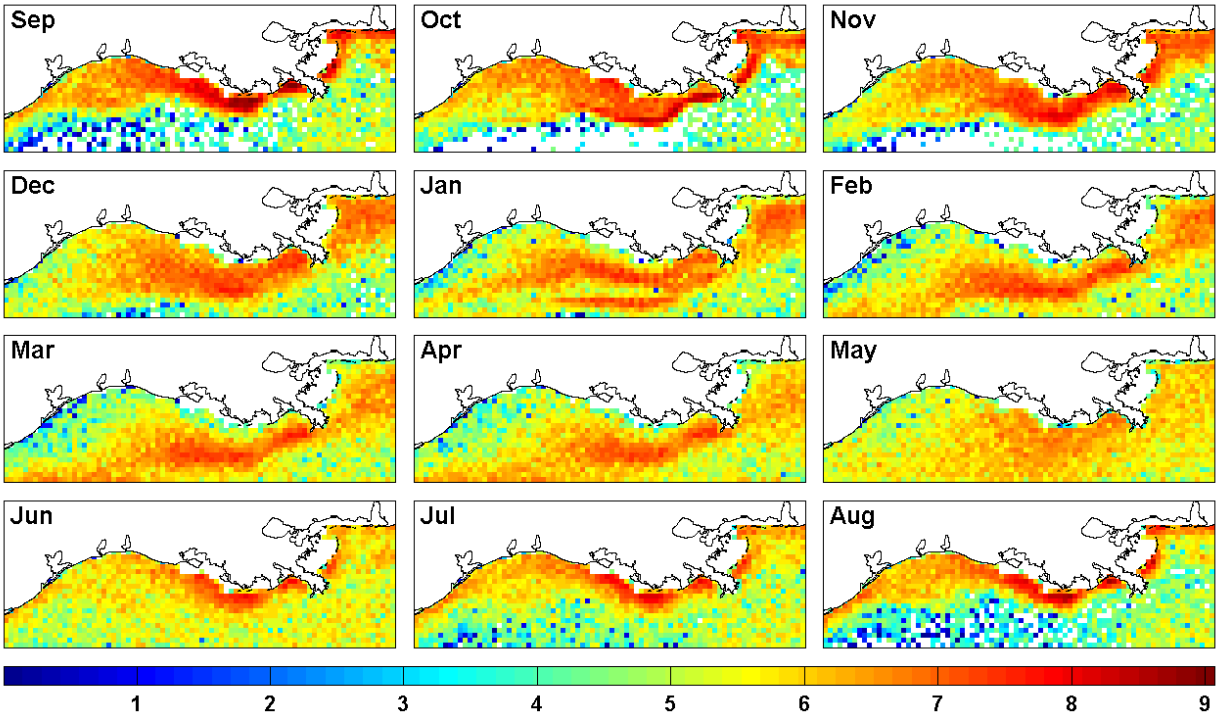

Figure 11: Mid-monthly snapshots showing the spatial distribution of age-2 adults in model year 95 from baseline run. Colored pixels represent the ln-transformed number of age-2 adults in a 10 x 10 cell area on the grid. Note figures 7-11 all show the same cohort.

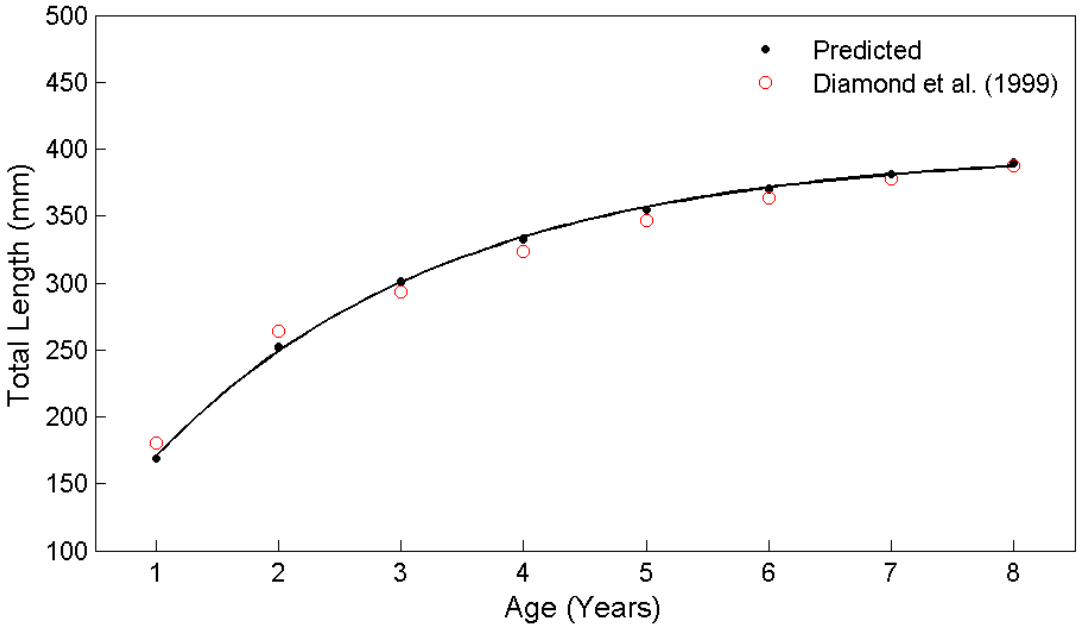

Figure 12: Simulated length-at-age under baseline conditions. Predicted mean beginning lengths (solid black circles) and fitted von Bertalanffy growth curve, $TL = 399.37 \cdot [1 - e^{-0.42 \cdot (age + 0.32)}]$, are shown for model years 61-100. Transformed beginning standard lengths ($TL = SL \cdot 1.25$) estimates from Diamond et al. (1999) are shown as red circles.

Spawning peaked around October 1 and ended, on average, by the end of March in the calibrated baseline simulation. Fraction mature was based upon length, and approximately 64% of age-1 individuals were mature each year; all individuals were mature by age-2. Age-2 and age-3 individuals accounted for more than 40% of total annual egg production (Table 6). Averaged eggs per gram was lowest for age-1 due to greater influence of the negative y-intercept term (-3248 in equation 6) and leveled off by age-4. Averaged eggs per individual was very low for age-1 because not all age-1 individuals were mature (immature individuals were still included in the denominator), and averaged eggs per individual increased steadily with age for age-2 through age-7 because fecundity increased with body weight. Average total annual egg production for years 61-100 was 360 billion. Average number of individuals entering age-1 was 1.5 million during years 61-100, and average age-2 and older abundance was 1.7 million. The average year-end abundance of age 2 and older individuals for years 61-100 was 1.08 million.

Table 6: Contribution to total annual egg production by each age class as percent of total egg production (PTEP), potential spawning stock biomass (SSB) in metric tons of female weight present on September 1st, eggs per gram (EPG), and eggs per individual (EPI) in the baseline and severe simulations. Note the EPG and EPI were computed on a per batch basis. Values are reported as averages for years 61-100.

Age	Baseline				Severe			
	PTEP	SSB	EPG	EPI	PTEP	SSB	EPG	EPI
1	7.3	25.5	93.8	6416	8.0	18.6	93.5	6507
2	20.1	57.7	96.5	19717	19.8	40.9	92.0	18814
3	21.6	64.7	97.0	32826	20.9	44.6	93.4	31397
4	18.7	57.0	97.3	43927	18.8	39.3	97.2	43605
5	14.4	44.6	97.4	52647	14.5	30.8	97.4	52278
6	10.5	32.6	97.4	59209	10.6	22.5	97.4	58859
7	7.3	22.9	97.4	64030	7.4	15.8	97.4	63721

Hypoxia Effects: Mild, Intermediate, and Severe

Repeated exposure to low DO year after year resulted in small declines in population abundance for the mild and intermediate scenarios and a larger decline for the severe scenario. Average age-2 and older abundance for years 61-100 were 97% of baseline for mild hypoxia, 94% of baseline for intermediate hypoxia, and 69% of baseline for severe hypoxia (Figure 13). Relative abundances were consistent across life stages in all three simulations (mild, intermediate, and severe). The range of percent baseline abundance for years 61-100 across all stages was 68-70% for the severe scenario, compared to 69% for age-2 and older abundance.

Hypoxia Effects: Detailed Examination of Severe Results

Avoidance behavior resulted in age-1 and older individuals concentrating in areas just outside of the hypoxic area (Figure 14). Peak cell abundance was higher in the severe scenario compared to baseline (Figure 14). The general spatial-abundance distributions in other months were similar to baseline.

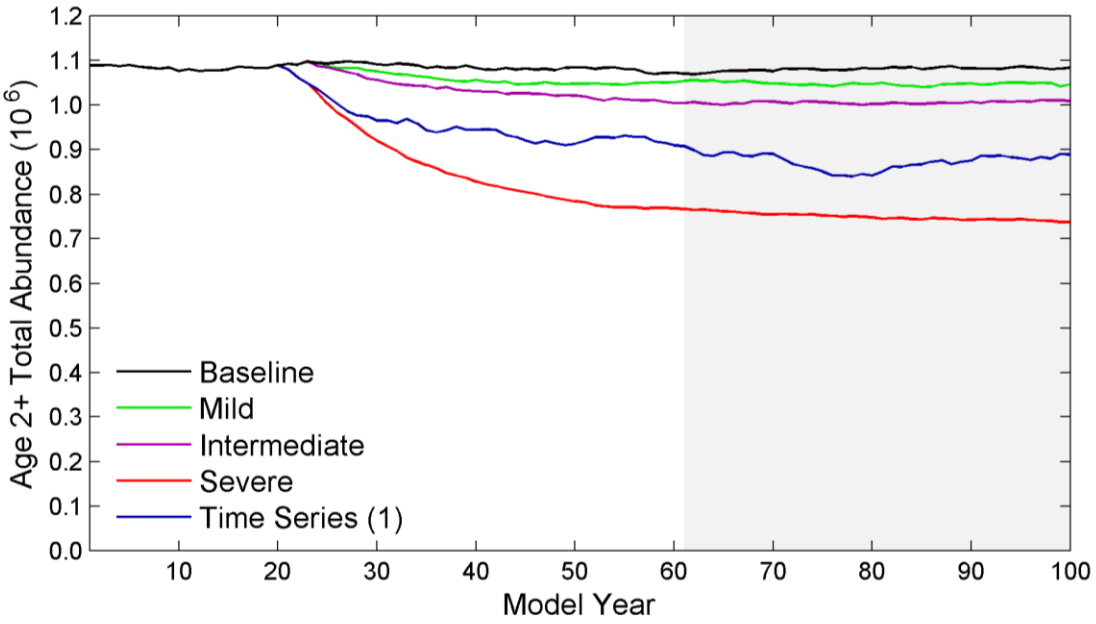

Figure 13: Age 2 and older abundance for baseline, mild, intermediate, severe, and time series (replicate number one) simulations. Shading area demarcates the last 40 model years (61-100).

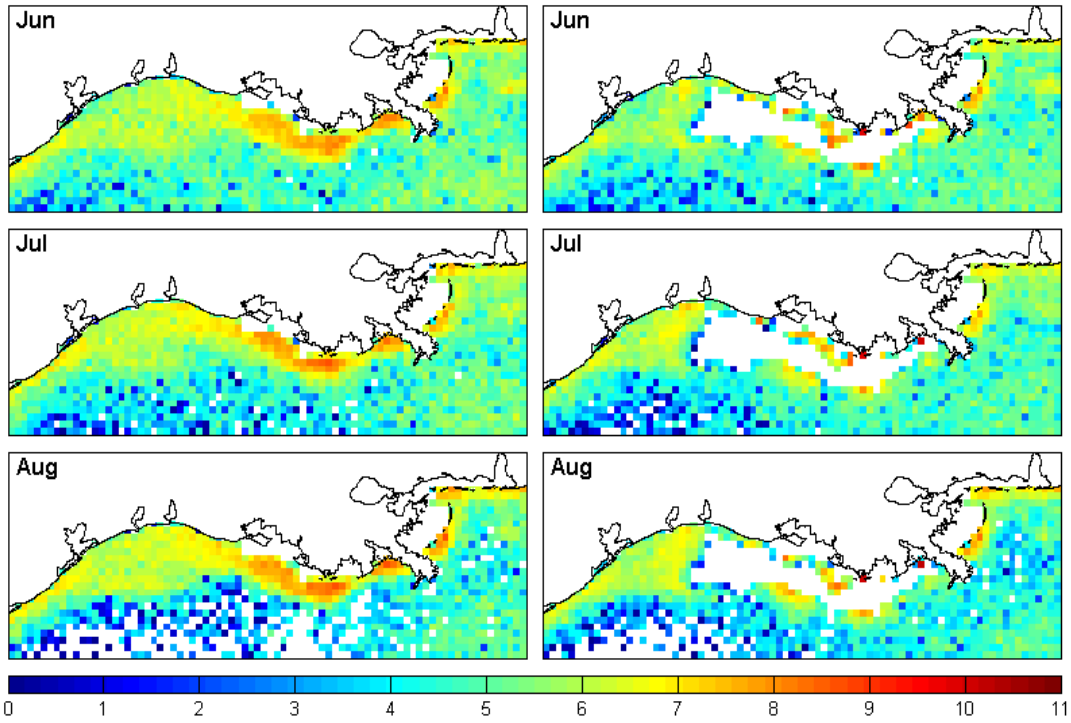

Figure 14: Mid-monthly snapshots showing the spatial distribution of age-2 individuals in model year 95 from the baseline (left column) and severe hypoxia (right column) simulations. Colored pixels represent the ln-transformed number of age-2 individuals in each area that is the sum of a 10 x 10 set of model cells.

A small percent of individuals in the population were exposed to hypoxia each year. The percent of age-0 (late juveniles and remaining early juveniles), age-1, and age-2 individuals exposed to DO < 4.0 mg/L peaked around June 7 (Figure 15a), during the period of time hypoxia was setting up (linearly decreasing from normoxia) in the cells. Once individuals either died or avoided the initial set-up of hypoxia, the percent exposed dropped and stayed at 4-5% throughout the remainder of the hypoxic period. The percent of age-1 and age-2 individuals exposed to DO < 4.0 mg/L (Figure 15c) was about 5 times that of age-0 individuals (Figure 15b). Relatively few individuals were exposed to DO < 1.5 mg/L, and it only occurred for few days as hypoxia set-up. Most individuals exposed to DO < 4.0 mg/L were exposed to DO between 1.25 and 3.0 mg/L. While the percent of individuals exposed on any given hour was low, many individuals were exposed over time. The average percent of surviving age-1 and age-2 individuals on September 1 of each year that ever experienced at least one hour of DO < 4.0 mg/L during the just past summer were 23% and 60% for years 61-100.

While a small percent of individuals in the population were exposed, exposed individuals showed significant reductions in their hourly growth, reproduction, and survival (Figure 16). On average, hourly growth rates were reduced by more than 90% (Vg < 0.1) for the few days when age-0 to age-2 individuals were exposed to DO < 1.25 (Figure 16a). Survival was also reduced during this early period of hypoxia (Vs dipped to 0.8 briefly, Figure 16a). There was no effect on reproduction (Vg = 1) because the early period of hypoxia does not contribute to reproductive effects, which accumulate over the last 10 weeks of the hypoxia period. Individuals exposed to DO between 1.25 and 4.0 mg/L (Figure 16b-c) showed no survival effects (mortality occurs below 1.25 mg/L), very small growth effects, and an accumulating reduction in fecundity until fecundity of exposed individuals by September 1 was 80-85% of normoxic fecundity.

Low DO caused small, consistent reductions in survival and fecundity at the population level that resulted in the 31% reduction in average age-2 and older abundance (Figure 13). There were no detectable low DO effects on growth at the population level. Mean length-at-age in the severe hypoxia simulation showed little deviation from baseline. The change in age 1-8 beginning weights between the baseline and severe hypoxia simulations were all less than 2%.

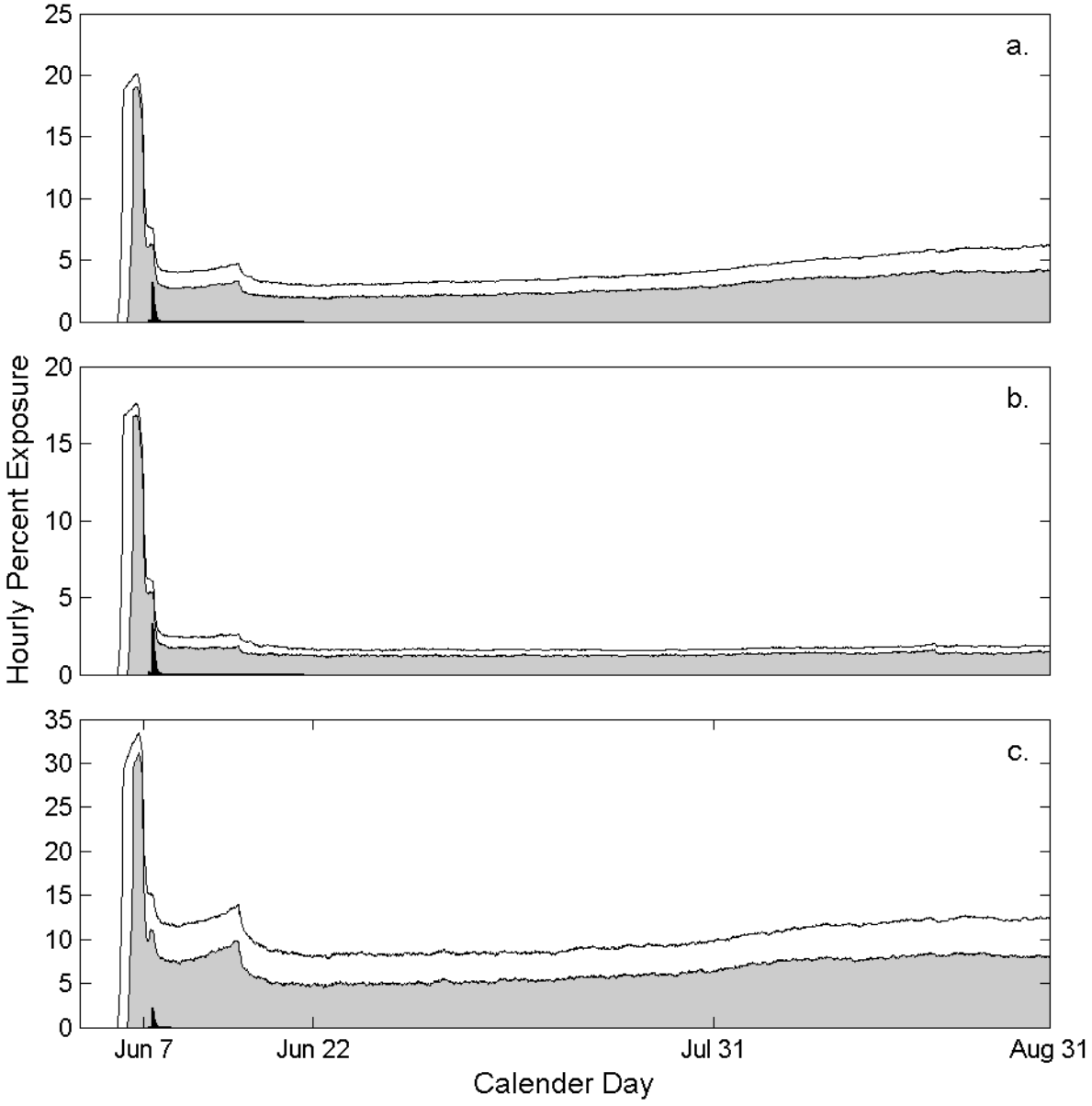

Figure 15: Stacked area plot showing percent exposure to 3.0 ≤ DO < 4.0 mg/L (▭), 1.25 ≤ DO < 3.0 mg/L (▭), and DO < 1.25 mg/L (■) each hour in model year 95 in the severe hypoxia simulation for (a) age 0-2 , (b) age-0 only, and (c) age 1-2 only.

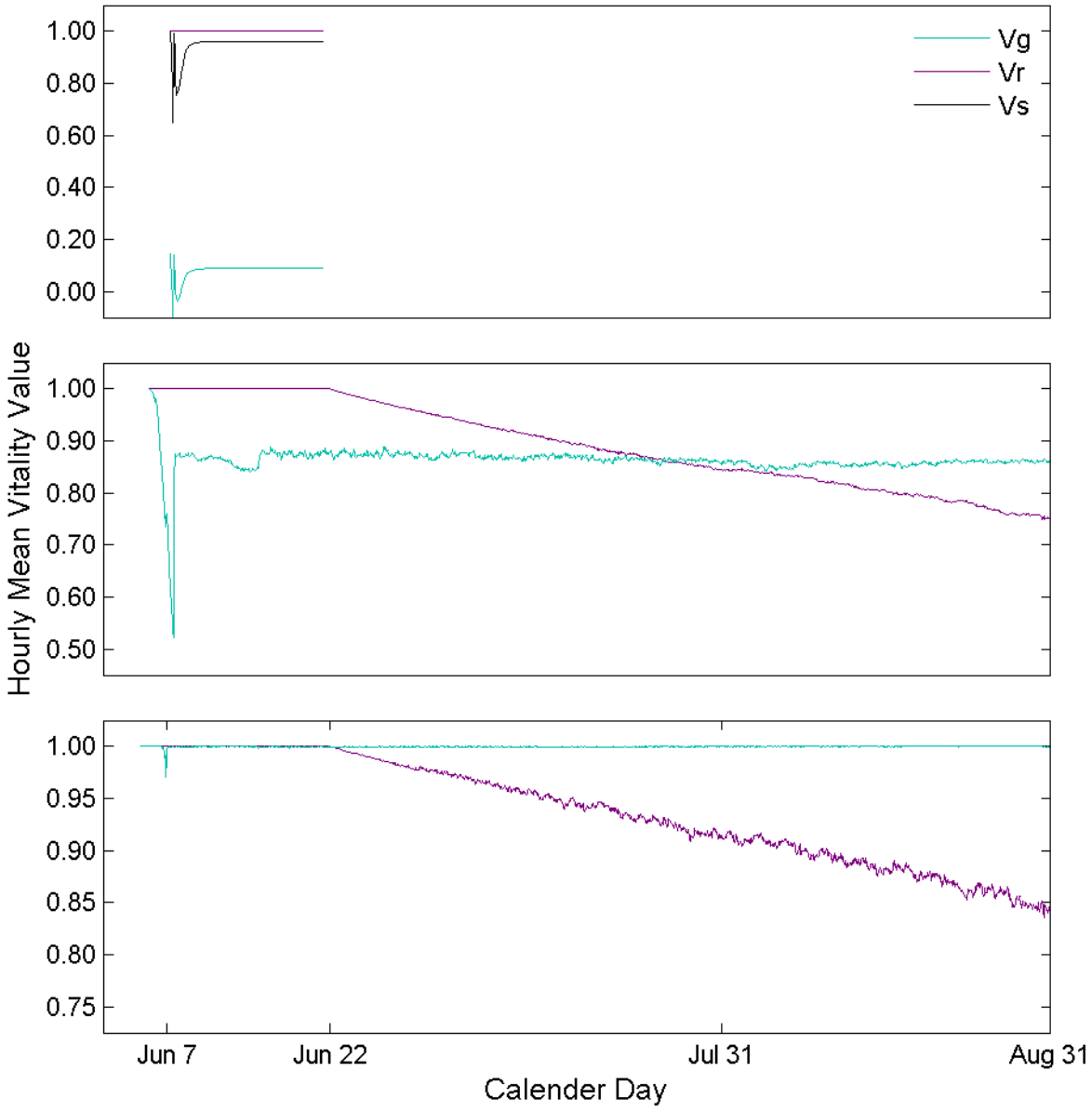

Figure 16: Hourly mean vitality values from June 1 to August 31 for individuals exposed to (a) DO < 1.25 mg/L, (b) 1.25 ≤ DO < 3.00 mg/L, and (c) 3.00 ≤ DO < 4.00 mg/L in model year 95 in the severe hypoxia simulation.

Direct mortality due to hypoxia removed a small percent of individuals and reduced fecundity lowered the eggs per individual of spawners. Average daily mortality rate over years 61-100 for age-1 individuals increased from 0.0011 d^{-1} under baseline to 0.0012 d^{-1} in the severe simulation; for age-2 individuals increased from 0.0012 d^{-1} under baseline to 0.0013 d^{-1} in the severe simulation. The increase (< 0.3%) in age-0 mortality was negligible, as it was confounded by density-dependent changes in late juvenile mortality rate; survival of age-3 and older individuals was not affected by DO conditions. Eggs per gram and eggs per individual for age-2 and age-3 individuals decreased by about 5% from baseline values (Table 6). These small changes in mortality and fecundity compounded over the 80 years of repeated severe hypoxia conditions. Density-dependent mortality in the late juvenile stage offset some of the increased mortality and reduced fecundity from hypoxia (Figure 17). The population declined slowly each year as late juvenile mortality gradually decreased from 0.0171 d^{-1} in year 20 to an average rate in years 61-100 of 0.0165 d^{-1}. Once the increased mortality and reduced fecundity from hypoxia was offset by the decreased late juvenile mortality rate, the population reached a new equilibrium abundance at about 69% of the baseline abundance (Figure 13).

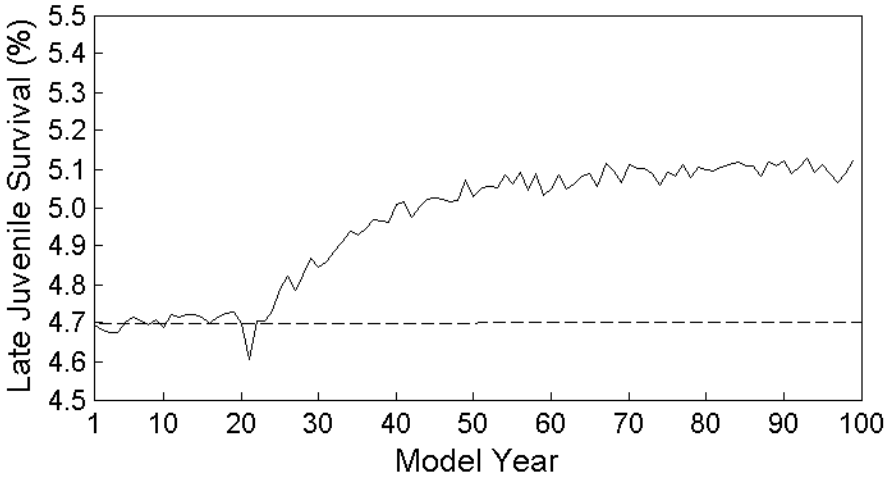

Figure 17: Late juvenile stage survival in the severe hypoxia simulation. Average late juvenile stage survival during years 61-100 under baseline conditions shown (dashed line) for reference

Hypoxia Effects: Time Series Simulations

When hypoxia was simulated as a random time series of mild, intermediate, and severe years, the average age 2 and older abundance for years 61-100 ranged from 71 to 82% of baseline average abundance across 12 replicates (Figure 18). The variation in the percent of baseline abundance was due to the effects of different sequences of mild, intermediate, and severe hypoxia years within each replicate simulation (Figure 19). The expected percent of age-2 and older baseline abundance based on the frequency of occurrence in the time series simulations was 82% (0.12 x 96% + 0.40 x 94% + 0.42 x 69%), corresponding to average age-2 and older abundance of approximately 0.89 million. Percent baseline abundance was less than the expected for the majority of replicates; median percent baseline abundance was 74%.

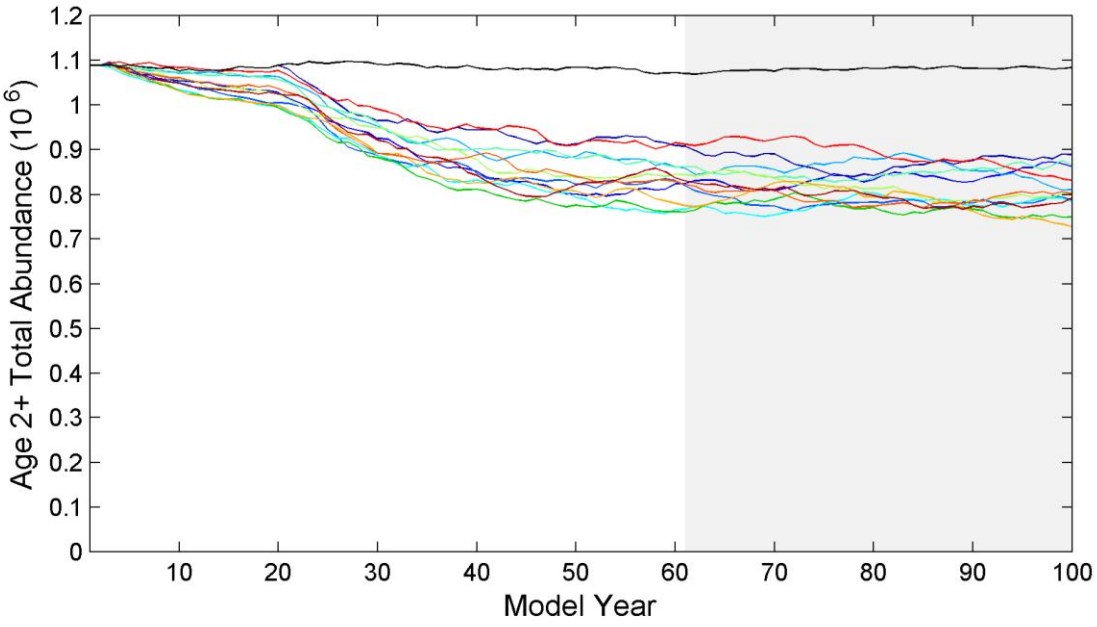

Figure 18: Total abundance of age-2 and older individuals in the 12 time series replicates, original baseline (black line) age-2 and older total abundance included for reference. Shaded area demarcates the last 40 years (61-100).

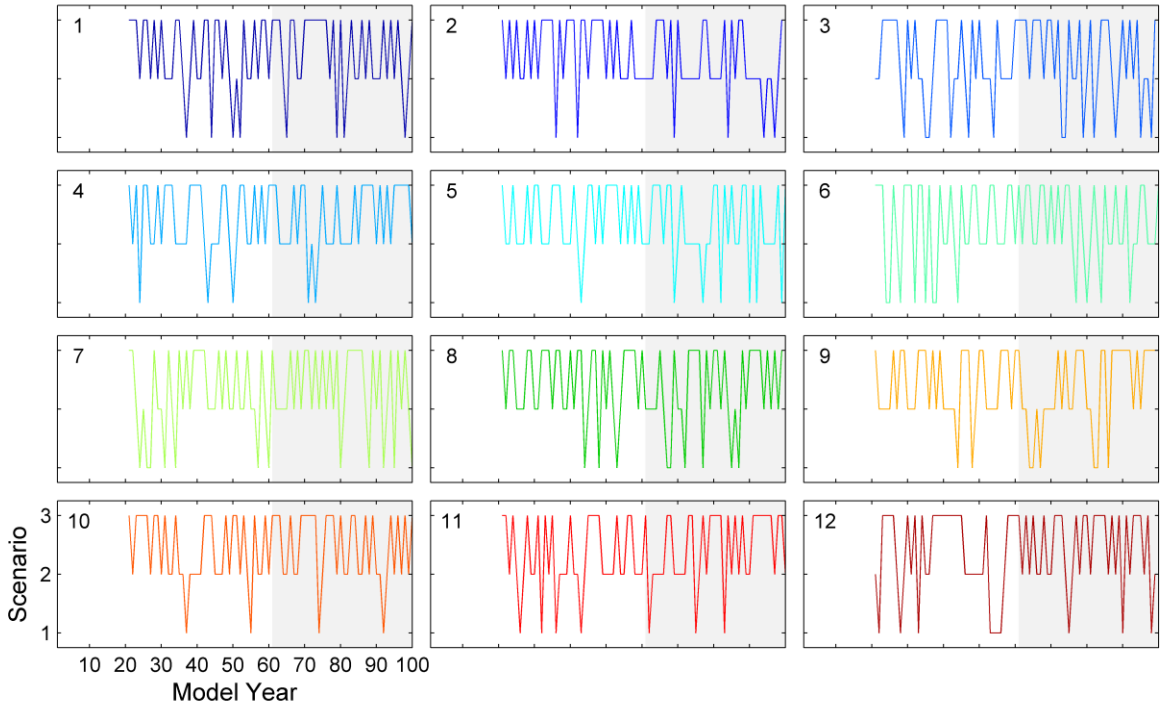

Figure 19: The 12 scenario sequences (1 = mild, 2 = intermediate and 3 = severe) used for the replicate runs of the time series simulation. Number for the corresponding times series replicate shown in the upper left hand corner of each panel. Shaded area demarcates years 61-100.

The effects of the proportion of mild versus severe hypoxia years in each replicate simulation were not obviously related to the predicted reductions in population abundance, but the effects of short sequences of severe or mild conditions were reflected in short-term changes in population abundance. The percent of baseline abundance was uncorrelated to the proportion of mild (r^2 = -0.5609, n = 12, $p > 0.05$) or to the proportion of severe years (r^2 = -0.0301, n = 12, $p > 0.05$) during years 61-100. However, there were several contiguous years of either severe or mild-intermediate DO conditions within replicates runs that produced short-term trends in population abundance. For example, years 70 to 80 in replicate 1 had mostly severe conditions and age 2 and older abundance during this period steadily declined from 0.89 million to 0.84 million. Years 70 to 80 in replicate 5 had all mild or intermediate hypoxia conditions and age 2 and older abundance during these years steadily increased from 0.75 million to 0.80 million.

Sensitivity Analysis

Model predictions under time series conditions (replicate 6) were sensitive to both the number of cells individuals were allowed to search and the DO level that triggered avoidance (simulations A-E in Figure 20). For a given trigger value, percent of baseline abundance decreased by as much as 28% from the 80-cell search to the 24-cell search. For example, percent of baseline abundance was 82% for the 80-cell search (original replicate 6) and 65% for the 24-cell search with a trigger of 2.0 mg/L. Similar reductions were predicted between 80 and 24 cell searches for the 1.5 mg/L trigger and for the 2.5 mg/L trigger.

A similar effect was predicted for the trigger between 2.0 and 1.5 mg/L, but smaller effects were predicted for the trigger between 2.0 and 2.5 mg/L. For example, percent of baseline abundance went from 82% to 63% under the 80-cell search when the trigger was reduced from 2.0 mg/L to 1.5 mg/L, while only a slight increase in percent of baseline abundance (82% to 84%) was predicted under the 80-cell search when trigger was increased from 2.0 mg/L to 2.5 mg/L. Similar patterns of changes in abundance across the trigger values were predicted with the 24-cell search.

The predicted reduction in age-2 and older abundance was due to the combined effects of low DO effects on survival and reproduction, with growth effects playing a smaller role (simulations F-H in Figure 20). When only mortality was affected by low DO, predicted age-2 and older abundance was 90% of baseline. The fecundity effect alone was 92%, while the growth effect alone was 95%. The product of these reductions is 0.78, which is similar to the original replicate 6 time series simulation (82%). Furthermore, predicted baseline abundance with growth effects removed was also similar (84%), demonstrating that growth effects were small.

Avoidance movement was moderately sensitive to mixing and to cues used to select the destination cells. Average age-2 and older abundance was 73% of baseline when episodic mixing events were imposed in June, July, and August (simulation M, Figure 20). The lowered average abundance under mixing was due to individuals getting exposed to DO < 1.25 mg/L every time hypoxic conditions were re-established after a mixing event. Average age-2 and older abundance was 67% of baseline when individuals simply moved to the cell with the highest DO (simulation N, Figure 20), rather than selecting the cell with the best temperature among cells with DO > 2.0 mg/L.

The predicated age-2 and older abundance was also moderately sensitive to the number of age-classes affected by low DO. Predicted age-2 and older abundance when all ages (0-8) were affected by low DO was 73% of baseline (simulation L, Figure 20). A moderate decline was expected when all ages were affected because age-2 individuals constituted about 40% of the age-2 and older population and age-3 fecundity, which accounted for a large proportion of annual egg production (Table 6), was already affected by low DO in the time series simulations.

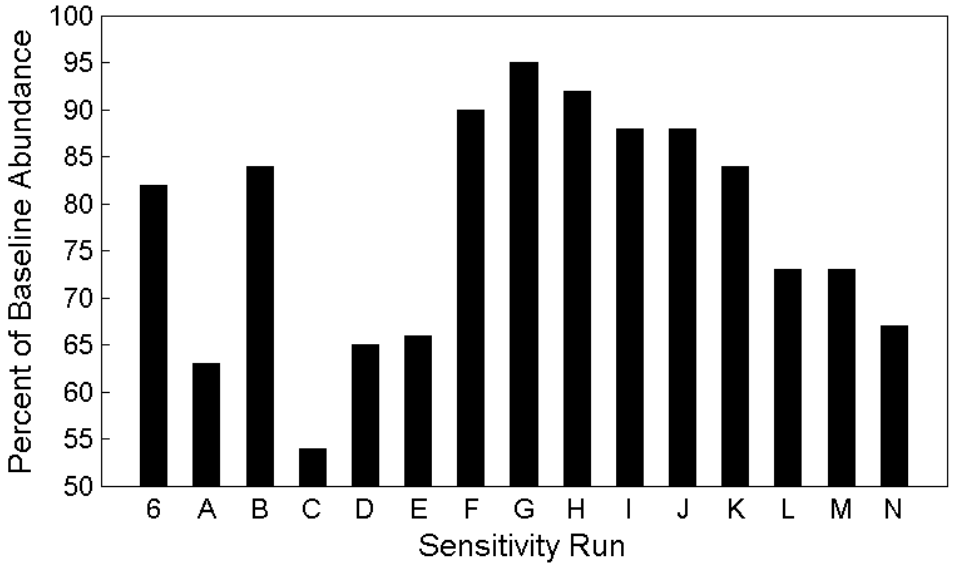

Figure 20: Percent of recomputed baseline abundance for sensitivity runs described in Table 5. The percent of recomputed baseline abundance from time series replicate 6 shown for reference.

DISCUSSION

Effects of Hypoxia

A spatially-explicit, individual-based model was used to isolate and analyze possible direct effects of hypoxia on Atlantic croaker population dynamics in the northwestern Gulf of Mexico. The hourly growth, mortality, reproduction, and movement of individual croaker from fertilization until age-8 for 100 years were followed on a 2-dimensional spatial grid. The daily environmental conditions (temperature, chlorophyll-a, DO) were specified for each cell in the grid based on average conditions, and these average conditions were repeated year after year for 100 years. The strategy was to simulate quasi-realistic conditions for croaker but by repeating the same conditions every year, any long-term cumulative effects of hypoxia would be quantifiable. A more realistic set of conditions for simulating croaker population dynamics (i.e., realistic recruitment variability) would have been to have inter-annual differences in environmental conditions. Such variability would have made isolation of the hypoxia effects, especially any small to moderate effects, more difficult.

Under these repeated environmental conditions, 80 years of either mild or intermediate seasonal hypoxia produced small reductions in population abundance, while severe hypoxia caused a 31% reduction in long-term population abundance. The effects of severe hypoxia slowly built up in the model over years; population abundance slowly declined for about 40 years before the 31% reduction was realized. The average percent of baseline abundance in the severe hypoxia simulation following the 20-year spin-up was 92% over years 21-30, 80% over years 31-40, 73% over years 41-50, and 70% over years 51-60. Predicted low DO (< 4.0 mg/L) exposure for age-0, age-1, and age-2 croaker individuals on a per hour basis in the severe simulation was small (mostly about 5%), but a large proportion of age-0, age-1, and age-2

croaker (20-40%) were exposed to low DO at least once during the hypoxia season. The exposure history of age-1 and age-2 croaker had important implications on egg production in the model because they contributed to the spawning population in subsequent years. When the severe hypoxia condition was compounded annually over 80 years, the added daily mortality due to hypoxia incurred by age-1 (0.0012 d^{-1} versus 0.0011 d^{-1}; 9% higher) and age-2 (0.0013 d^{-1} versus 0.0012 d^{-1}; 8% higher) individuals, coupled with the 5% average reduction in eggs per individual in age-2 and age-3 croaker from exposure to DO < 4.0 mg/L throughout the summer period (Table 6), caused average annual egg production over years 61-100 to decrease from its baseline value of 360 billion to 246 billion. Age-1 and age-2 individuals had lowered fecundity, and the increased mortality of age-1 and age-2 individuals persisted into the older ages (fewer age-3 and older in later years) because mortality was density-independent for adults. The decrease in egg production was eventually offset by increased late juvenile survival, which was density-dependent, resulting in an equilibrium value for total abundance under the severe hypoxia scenario that was 69% of baseline.

Under more realistic hypoxia conditions of mild, intermediate, and severe hypoxia years occurring in proportion to their historical frequency, the model predicted an 18-29% decrease in the long-term (years 61-100) population abundance (Figure 18). There was no obvious relationship between the proportion of the 80 years that were mild or severe and population reduction among the replicate simulations. Within replicate runs, short periods of persistent mild or severe conditions did correspond to short-term increases or decreases in abundance.

I performed a sensitivity analysis to examine the influence of factors effected by hypoxia and the sensitivity of predicted abundance of age-2 and older croaker to modeled avoidance behavior. Predicted reductions in abundance were primarily due to the combined effects of low

DO on reproduction and survival, and were sensitive to assumptions concerning the avoidance behavior of Atlantic croaker. Predicted percent of baseline abundance from replicate 6 of the time series simulations was reduced from 82% to about 65% when either: (1) the number of cells searched was reduced from 80 to 24 or (2) the DO threshold at which the avoidance response was triggered was reduced from 2.0 mg/L to 1.5 mg/L (Figure 20, sensitivity runs A and D). Increasing the avoidance trigger from 2.0 mg/L to 2.5 mg/L for either the 80 or 24 cell search did not produce an appreciable change in predicted percent of baseline abundance (Figure 20, sensitivity runs B and E). These results indicate individuals were proficient at avoiding hypoxia when allowed to move up to 6.4 km in 1 hour, which is at the upper limit of reported swimming speeds.

Survival, reproduction, and growth effects acted in a roughly additive manner (Figure 20, sensitivity runs F-H). Survival alone resulted in an abundance that was 90% of baseline, reproduction alone resulted in 92% of baseline, and growth alone resulted in 95% of baseline. Their product (78%) was similar to the percent of baseline obtained (82%) with the time series simulation. Growth effects played the smallest role. The small growth effect produced in the model can be explained by the narrow range of DO concentrations (0.58-3.0 mg/L) over which the vitality-repair sub-model for growth operated, which was combined with only short exposure that affected growth once individuals were able to avoid cells with DO < 2.0 mg/L.

One indirect effect that was present in the model was the displacement of croaker from hypoxic areas (e.g., Figure 14). Individuals, primarily late juveniles, constrained to areas along the inshore edge of the hypoxic zone in the severe simulation occupied vicinities on the grid with near optimal temperature and high chlorophyll-a values, conditions in the model conducive to higher growth rates. Individuals, mostly age-1 and older croaker, located along the seaward edge

of the hypoxic zone occupied areas with both colder temperature and lower chlorophyll-a values, which could result in slower growth. Craig and Crowder (2005) noted a similar displacement pattern for croaker collected in annual bottom trawl surveys that were conducted during June-July along the western part of the Louisiana continental shelf from 1987-2000. In the simulations presented here, the indirect effects of displacement to due hypoxia avoidance did not result in significantly slowed growth at the population level. In the severe hypoxia simulation, the combined direct effects of low DO on growth and the indirect effects from displacement resulted in beginning weights at age and percent of age-1 mature within 2% of baseline values. There are likely other environmental conditions that could be used in the model that would result in the direct and indirect effects on growth to be larger. A simulation in which growth, reproduction, and mortality were unaffected by low DO but individuals still avoided hypoxia would also be interesting. In the sensitivity analysis, when individuals simply searched 80 surrounding cells for the highest DO regardless of water temperature, the percent of baseline was 67% (sensitivity run N), compared to 82%, suggesting that indirect effects of temperature on growth are possible in the model.

Some Model Strengths and Weaknesses

The model adequately simulated exposure to low DO (DO < 4.0 mg/L) and provided reasonable estimates of its relative effects on growth, reproduction, and survival. The goal was to develop the spatially-explicit, individual-based model in order to isolate any long-term effects of hypoxia. Simulating exposure is therefore critical. Exposure depends on the realism of the spatial and temporal dynamics of the low DO on the grid, the realism of the movement patterns of the individuals, and then how these time-varying exposures get translated into effects on survival, reproduction, and growth. The mild, intermediate, and severe hypoxia scenarios

simulated were based on observed hypoxia from field surveys. Kinesis movement with avoidance behavior produced reasonable spatial distributions. Whether the appropriate numbers of individuals in the population were exposed to low DO levels, and individuals experienced realistic exposure over time, remains debatable. The effects sub-models that used vitality were developed and tested using laboratory data outside of the information used in the individual-based model and thus should be fairly robust.

The model also had several major weaknesses. Almost every aspect of the model could be criticized simply because it is a model based on incomplete information. I highlight some of the major weaknesses here. Density-dependent survival was represented only in the late juvenile stage; if density-dependence occurs in other stages or is weaker or stronger than I assumed, the predicted effects of hypoxia could change. Natural mortality rates were assumed constant over time and throughout the spatial grid. I also assumed mortality due to hypoxia was not represented in the total mortality rates used as model inputs; mortality in the mild, intermediate, and severe simulations included the calibrated baseline mortality plus the added mortality incurred due to hypoxia. Thus, the mortality rates in the model simulations may be too high. However, the model was calibrated to generate a stable population without hypoxia so the predicted declines in abundance, relative to baseline, should be robust. The effects of hypoxia in the model were influenced by losses of age-1 and age-2 individuals persisting through the older ages. If adult mortality was density-dependent or varied substantially for other reasons, the compounding effects of losses of age-1 and age-2 could be diminished. One can always argue about exposure and avoidance, as these were critical in the simulations, but also based on the relatively little empirical information. Avoidance behavior also ignored any vertical movements. Finally, the environmental conditions simulated in the model represented average conditions for

the NWGOM. Temperature and chlorophyll-a were repeated year after year, and the hypoxia scenarios were not linked to temperature or chlorophyll-a conditions in the model. Finally, DO values were assumed uniform within the grid cells (i.e., small-scale variability was ignored).

Future Directions

The present individual-based model can be used for further exploration of the hypoxia effects on croaker population dynamics. More realistic environmental conditions can be simulated by varying the environmental conditions from year to year. Knowing how hypoxia effects manifest in the model, it is possible to isolate the population effects of hypoxia with the croaker population dynamics showing more realistic inter-annual variability. Another area for future exploration with the model is to link the hypoxia conditions with the chlorophyll-a conditions in the model, as both are related to Mississippi River flow (Justic et al. 1993, Walker and Rabalais 2006). Also, more realistic hypoxia scenarios can be simulated that include mixing and fine-scale (sub-grid cell scale) variability. The spike in hourly exposure to DO < 1.5 mg/L that occurred just after low DO conditions setup in the severe simulation (Figure 15) was likely a result of the way the lowering DO conditions were simulated in the model. DO observations on the scale of seconds and meters are available (Michael Roman, unpublished data) that show that DO can vary ±1-2 mg/L on fine temporal and spatial scales (i.e., within a single model cell). This variability can be implemented in the model by generating unique DO values to each individual in a grid cell each hour assuming the DO value of the grid cell in our scenarios is the mean value.

Additional computer simulation studies are needed to better assess the DO exposure of Atlantic croaker in the NWGOM. An existing high resolution, 3-D hydrodynamics model for the Louisiana-Texas shelf (Wang and Justic 2009) coupled with an NPZ sub-model (e.g., Ji et al.

2008a, b) could be used in future modeling efforts to better simulate water quality. Using the 3-D hydrodynamics model, "smart particle" tracking experiments in which croaker are represented as Lagrangian particles imparted with avoidance behavior could then be used estimate DO exposure under more dynamic environmental conditions that include the vertical dimension. The 3-D model cannot be used to simulate 100 years but can be used in shorter simulations to examine the 3 to 4 month summertime period. Alternative movement algorithms to the kinesis used in the individual-based model can be implemented in the 3-D model to determine how they would affect exposure, and aspects of behavior, such as vertical avoidance of DO ignored in the individual-based model, can be investigated in the 3-D model. Dynamically changing DO conditions would create more realistic conditions and likely highlight weaknesses and allow refinement of the avoidance behavior used in the individual-based model.

Another area for future research is to compare simulated exposure patterns to those measured in the field in an ongoing study. The modeling analysis presented here is part of larger, long-term project that includes a major laboratory and field-monitoring component. Thomas and Rahman (2009) report on the potential of a particular biomarker (HIF, hypoxia-inducible factor) in ascertaining the exposure history of individual croaker collected from hypoxic sites. The transcription rate of HIF mRNA, and its subsequent protein expression, is upregulated under low DO conditions, possibly providing a reliable dose-response type relationship of exposure for field-caught croaker. Laboratory experiments are underway to establish a clear relationship between HIF mRNA expression and exposure history. In 2010, croaker was collected from across the Louisiana Shelf using the same grid of stations as is used for the annual hypoxia monitoring as part of the NOAA/CSCOR Gulf of Mexico Ecosystems and Hypoxia Assessment Program. Fecundity and HIF were measured in these fish, as well as in

control areas. These data, once available, will be compared to model-predicted exposures and fecundity reductions. Also, as part of this long-term project, the summer SEAMAP data are being analyzed to estimate the proportion of the croaker exposed to low DO (Kevin Craig, personal communication). The summer SEAMAP surveys are conducted on the Louisiana shelf and are being used to reconstruct the historical exposure of croaker for years 1987-2008. Finally, croaker will be tagged and tracked in the summer of 2011 using telemetry methods and will be followed as individual tracks as individuals move into and out of the local hypoxia conditions (Thomas Grothues, personal communication). All of these field and laboratory data will become available over the next year and will provide a strong empirical basis for evaluating the exposure patterns simulated in the individual-based model and potentially in any 3-D simulations.

LITERATURE CITED

Arnoldi, D. C., Herke, W. H., and Clairain, E. J. Jr. 1973. Estimate of growth rate and length of stay in a marsh nursery of juvenile Atlantic croaker, *Micropogon undulates* (Linnaeus), "sandblasted" with fluorescent pigments. Proceedings of the Gulf and Caribbean Fisheries Institute. 26: 158-172.

Baltz, D. M. and Jones, R. F. 2003. Temporal and spatial patterns on microhabitat use by fishes and decapod crustaceans in a Louisiana Estuary. Transactions of the American Fisheries Society. 132(4): 662-678.

Barger, L. E. 1985. Age and growth of Atlantic croakers in the northern Gulf of Mexico, based on otolith sections. Transactions of the American Fisheries Society. 114(6): 847-850.

Baustian, M. M., Craig, J. K., and Rabalais, N. N. 2009. Effects of summer 2003 hypoxia on macrobenthos and Atlantic croaker foraging selectivity in the northern Gulf of Mexico. Journal of Experimental Marine Biology and Ecology. 381: S31-S37.

Benhamou, S. and Bovet, P. 1989. How animals use their environment: a new look at kinesis. Animal Behaviour. 38(3): 375-383.

Breitburg, D. L. 1992. Episodic hypoxia in Chesapeake Bay: Interacting effects of recruitment, behavior, and physical disturbance. Ecological Monographs. 62(4): 525-546.

Brietburg, D. L. 2002. Effects of hypoxia, and the balance between hypoxia and enrichment, on coastal fishes and fisheries. Estuaries. 25(4b): 767-781.

Breitburg, D. L., Craig, J. K., Fulford, R. S., Rose, K. A., Boynton, W. R., Brady, D. C., Ciotti, B. J., Diaz, R. J., Friedland, K. D., Hagy III, J. D., Hart, D. R., Hines, A. H., Houde, E. D., Kolesar, S. E., Nixon, S. W., Rice, J. A., Secor, D. H., and Targett, T. E. 2009a. Nutrient enrichment and fisheries exploitation: interactive effects on estuarine living resources and their management. Hydrobiologia. 629: 31-47.

Breitburg, D. L., Hondorp, D. W., Davias, L. A., and Diaz, R. J. 2009b. Hypoxia, nitrogen, and fisheries: integrating effects across local and global landscapes. Annual Review of Marine Science. 1: 329-349.

Caddy, J.F. 1993. Toward a comparative evaluation of human impacts on fishery ecosystems of enclosed and semi-enclosed areas. Reviews in Fisheries Science. 1: 57-95.

Caddy, J. F. 2000. Marine catchment basin effects versus impacts of fisheries on semi-enclosed seas. ICES Journal of Marine Science. 57: 628-640.

Chan, F., Barth, J. A., Lubchenco, J., Kirincich, A., Weeks, H., Peterson, W. T., and Menge, B. A. 2008. Emergence of anoxia in the California current large marine ecosystem. Science. 319: 920.

Cheek, A. O., Landry, C. A., Steele, S. L., and Manning, S. 2009. Diel hypoxia in marsh creeks impairs the reproductive capacity of estuarine fish populations. Marine Ecology Progress Series. 392: 211-221.

Chesney, E. J. and Baltz, D. M. 2001. The effects of hypoxia on the northern Gulf of Mexico coastal ecosystem: a fisheries perspective. *In* Coastal Hypoxia: Consequences for Living Resources and Ecosystems. Ed. Rabalais, N. N., and Turner, R. E. Coastal and estuarine studies 58, American Geophysical Union, Washington, D.C.

Chesney, E. J., Baltz, D. M., and Thomas, R. G. 2000. Louisiana estuarine and coastal fisheries and habitats: perspective from a fish's eye view. Ecological Applications. 10(2): 350-366.

Chittenden, M. E. Jr. and Moore, D. 1977. Composition of the ichthyofauna inhabiting the 110-meter bathymetric contour of the Gulf of Mexico, Mississippi River to the Rio Grande. Northeast Gulf Science. 1: 106-114.

Cloern, J. E. 2001. Our evolving conceptual model of the coastal eutrophication problem. Marine Ecology Progress Series. 210: 223-253.

Conley, D. J., Cartensen, J., Vaquer-Sunyer, R., and Duarte, C. M. 2009. Ecosystem thresholds with hypoxia. Developments in Hydrobiology. 207: 21-29.

Cowan, J. H. Jr., Rose, K. A., and DeVries, D. R. 2000. Is density-dependent growth in young-of-the year fishes a question of critical weight? Reviews in Fish Biology and Fisheries. 10: 61-89.

Cowan, J. H. Jr., Grimes, C. B. and Shaw, R. F. 2008. Life history, history, hysteresis and habitat changes in Louisiana's coastal ecosystem. Bulletin of Marine Science. 83(1): 197-215.

Craig, J.K. and Crowder, L. B. 2005. Hypoxia-induced habitat shifts and energetic consequences in Atlantic croaker and brown shrimp on the Gulf of Mexico shelf. Marine Ecology Progress Series. 294: 79-94.

de Leiva Moreno, J. I., Agostini, V. N., Caddy, J. F., and Carocci, F. 2000. Is the pelagic-demersal ratio from fishery landings a useful proxy for nutrient availability? A preliminary data exploration for the semi-enclosed seas around Europe. ICES Journal of Marine Science. 57: 1091-1102.

Diamond, S. L., Crowder L. B., and Cowell, L. G. 1999. Catch and Bycatch: The qualitative effects of fisheries on population vital rates of Atlantic croaker. Transactions of the American Fisheries Society. 128(6): 1085-1105.

Diaz, R. J. and Rosenburg, R. 2008. Spreading dead zones and consequences for marine ecosystems. Science. 32: 926-929.

Eby, L. A., and Crowder, L. B. 2002. Hypoxia-based habitat compression in the Neuse River Estuary: context-dependent shifts in behavioral avoidance thresholds. Canadian Journal of Fisheries and Aquatic Sciences. 59: 952-965.

Eby, L. A., Crowder, L. B., McClellan, C. M., Peterson, C. H., and Powers, M. J. 2005. Habitat degradation from intermittent hypoxia: impacts on demersal fishes. Marine Ecology Progress Series. 291: 249-261.

GMFMC (Gulf of Mexico Fishery Management Council). 1980. Draft fishery management plan for groundfish in the Gulf of Mexico. GMFMC, Tampa, Florida.

Gregg, W. W., and Casey, N. W. 2004. Global and regional evaluation of the SeaWiFS chlorophyll data set. Remote Sensing of Environment. 93:463-479.

Grimes, C. B. 2001. Fishery Production and the Mississippi River discharge. Fisheries. 26(8): 17-26.

Hansen, D. J. 1969. Food, growth, migration, reproduction, and abundance of pinfish, *Lagodon rhomboides*, and Atlantic croaker, *Micropogon undulatus*, near Pensacola, Florida, 1963-65. Fishery Bulletin. 68: 135-146.

Hanson, P.C., Johnson T.B., Schindler, D. E., Kitchell, J. F., 1997. Fish bioenergetics 3.0 for Windows. Technical Report WISCU-T-97-001. University of Wisconsin Sea Grant Institute, Madison, WI, USA.

Hazen, E. L., Craig, J. K., Good, C. P., and Crowder, L. B. 2009. Vertical distribution of fish biomass in hypoxic waters on the Gulf of Mexico shelf. Marine Ecology Progress Series. 375: 195-207.

Houde, E. D. 2008. Emerging from Hjort's shadow. Journal of Northwest Atlantic Fisheries Science. 41: 53-70.

Humston, R., Olson, D. B., and Ault, J. S. 2004. Behavioral assumptions in models of fish movement and their influence on population dynamics. Transactions of the American Fisheries Society. 133(6): 1304-1328.

Ji, R., Davis, C., Chen, C., and Beardsley, R. 2008a. Influence of local and external processes on the annual nitrogen cycle and primary productivity on Georges Bank: A 3-D biological-physical modeling study. Journal of Marine Systems. 73:31-47.

Ji, R., Davis, C. S., Chen, C., Townsend, D. W., Mountain, D. G., and Beardsley, R. C. 2008b. Modeling the influence of low-salinity water inflow on winter-spring phytoplankton dynamics in the Nove Scotian Shelf-Gulf of Maine region. Journal of Plankton Research. 30(12): 1399-1416.

Justic, D., Rabalais, N. N., Turner, R. E., Wiseman Jr., W. J. 1993. Seasonal coupling between riverborne nutrients, net productivity and hypoxia. Marine Pollution Bulletin. 26(4): 184-189.

Kemp, W. M., Boynton, W. R., Adolf, J. E., Boesch, D. F., Boicourt, W. C., Brush, G., Cornwell, J. C., Fisher, T. R., Glibert, P. M., Hagy, J. D., Harding, L. W., Houde, E. D., Kimmel, D. G., Miller, W. D., Newell, R. I. E., Roman, M. R., Smith, E. M., and Stevenson, J. C. 2005. Eutrophication of Chesapeake Bay: historical trends and ecological interactions. Marine Ecology Progress Series. 303: 1-29.

Kitchell, J. F., Stewart, D. J., and Weininger, D. 1977. Applications of a bioenergetics model to yellow perch (*Perca flavescens*) and walleye (*Stizostedion vitreum vitreum*). Journal of the Fisheries Research Board of Canada. 34: 1922-1935.

Köster, F. W., Möllmann, C., Hinrichsen, H-H., Wieland, K., Tomkiewicz, J., Kraus, G., Voss, R., Makarchouk, A., MacKenzie, B. R., St. John, M. A., Schnack, D., Rohlf, N., Linkowski, T., and Beyer, J. E. 2005. Baltic cod recruitment – the impact of climate variability on key processes. ICES Journal of Marine Science. 62(7): 1408-1425.

McAllen, R., Davenport, J., Bredendieck, K., and Dunne, D. 2009. Seasonal structuring of a benthic community exposed to regular hypoxic events. Journal of Experimental Marine Biology and Ecology. 360(1): 67-74.

McNatt, R. A. and Rice, J. A. 2004. Hypoxia-induced growth rate reduction in two juvenile estuary-dependent fishes. Journal of Experimental Marine Biology and Ecology. 311(1) : 147-156.

Mississippi River/Gulf of Mexico Watershed Nutrient Task Force. 2008. Action Plan for Reducing, Mitigating, and Controlling Hypoxia in the Northern Gulf of Mexico and Improving Water Quality in the Mississippi River Basin. U.S. Environmental Protection Agency, Washington, D.C. (http://www.epa.gov/owow_keep/msbasin/actionplan).

Moore, D., Brusher, H. A., and Lee, T. 1970. Relative abundance, seasonal distribution, and species composition of demersal fishes off Louisiana and Texas, 1962-1964. Contributions in Marine Science. 15: 45-70.

Murphy, C. A., Rose, K. A., Rahman, M. S., and Thomas, P. 2009. Testing and applying a fish vitellogenesis model to evaluate laboratory and field biomarkers of endocrine disruption in Atlantic croaker (*Micropogonias undulates*) exposed to hypoxia. Environmental Toxicology and Chemistry. 28(6): 1288-1303.

Murphy, C. A. 2006. Modeling the effects of endocrine disrupting chemicals on Atlantic croaker: understanding biomarkers and predicting population responses. PhD dissertation, Louisiana State University, Baton Rouge.

Myers, R. A. and Cadigan, N. G. 1993. Density-dependent juvenile mortality in marine demersal fish. Canadian Journal of Fisheries and Aquatic Sciences. 50: 1576-1590.

National Research Council. 2008. The Mississippi River and the Clean Water Act: progress, challenges, and opportunities. National Academy Press, Washington, D.C.

Neilan, R. M., and Rose, K. A. (in prep). A mathematical model for growth, reproduction, and survival of fish and shrimp exposed to low dissolved oxygen.

Nixon, S. W. and Buckley, B. A. 2002. A strikingly rich zone – nutrient enrichment and secondary production in coastal marine ecosystems. Estuaries. 25: 782-796.

Nye, J. A. 2008. Bioenergetic and ecological consequences of diet variability in Atlantic croaker *Micropogonias undulatus* in Chesapeake Bay. Ph. D. Dissertation, University of Maryland, College Park.

Pihl, L., Baden, S. P., Diaz, R. J., and Schaffner, L. C. 1992. Hypoxia-induced structural changes in the diet of bottom-feeding fish and Crustacea. Marine Biology. 112: 349-361.

Rabalais, N. N. and Turner, R. E. 2001. Hypoxia in the northern Gulf of Mexico: description, causes and change. *In* Coastal Hypoxia: Consequences for Living Resources and Ecosystems. Ed. Rabalais, N. N., and Turner, R. E. Coastal and estuarine studies 58, American Geophysical Union, Washington, D.C. 1:1-36.

Rabalais, N. N., Turner, R. E., Sen Gupta., B. K., Boesch, D. F., Chapman, P., and Murrell, M. C. 2007. Hypoxia in the northern Gulf of Mexico: does the Science support the plan to reduce, mitigate, and control hypoxia? Estuaries and Coasts. 30(5): 753-772.

Rabalais, N. N., Turner, R. E., and Wiseman, W. J. Jr. 2002. Gulf of Mexico hypoxia, A.K.A. "The Dead Zone". Annual Review of Ecology and Systematics. 33: 235-263.

Rooker, J. R., Holt, S. A., Soto, M. A., and Holt, G. J. 1998. Postsettlement patterns of habitat use by sciaenid fishes in subtropical seagrass meadows. Estuaries and coasts. 21(2): 318-327.

Rose, K. A., Cowan, J. H. Jr., Winemiller, K. O., Myers, R. A., and Hilborn, R. 2001. Compensatory density dependence in fish populations: importance, controversy, understanding and prognosis. Fish and Fisheries. 2: 293-137.

Rose, K. A., Adamack,, A. T., Murphy, C. A., Sable, S. E., Kolesar, S. E., Craig, J. K., Breitburg, D. L., Thomas, P., Brouwer, M. H., Cerco, C. F., and Diamond, S. 2009. Does hypoxia have population-level effects on coastal fish? Musings from the virtual world. Journal of Experimental Marine Biology and Ecology. 381: S188-S203.

Ryther, J. H. 1969. Photosynthesis and fish production in the sea. Science. 166: 72-76.

Scheffer, M., Baveco, J. M., DeAngelis, D. L., Rose, K. A., and van Nes, E. H. 1995. Super-individuals a simple solution for modeling large populations on an individual basis. Ecological Modelling. 80: 161-170.

Shang, E. H. H., Yu, R. M. K., and Wu, R. S. S. 2006. Hypoxia affects sex differentiation and development, leading to a male-dominated population in zebrafish (*Danio rerio*). Environmental Science and Technology. 40(9): 3118-3122.

Sheridan, P. F., Trimm, D. L., and Baker, B. M. 1984. Reproduction and food habits of seven species of northern Gulf of Mexico fishes. Contribution in Marine Science. 77: 175-204.

Shimps, E. L., Rice, J. A., and Osborne, J. A. 2005. Hypoxia tolerance in two juvenile estuary-dependent fishes. Journal of Experimental Marine Biology. 325: 145-162.

Stierhoff, K. L., Targett, T. E., and Miller, K. Ecophysiological responses of juvenile summer and winter flounder to hypoxia: experimental and modeling analyses of effects on estuarine nursery quality. Marine Ecology Progress Series. 325: 255-266.

Stow, C. A., Qian, S. S., and Craig, J. K. 2005. Declining threshold for hypoxia in the Gulf of Mexico. Environmental Science and Technology. 39(3): 716-723.

Switzer, T. S., Chesney, E. J., and Baltz, D. M., 2009. Habitat selection by flatfishes in the northern Gulf of Mexico: implications for susceptibility to hypoxia. Journal of Experimental Marine Biology and Ecology. 381: S51-S64.

Thomas, P. and Rahman M. S. 2009. Biomarkers of hypoxia exposure and reproductive function in Atlantic croaker: A review with some preliminary findings from the northern Gulf of Mexico hypoxic zone. 381: S38-S50.

Thomas, P., Rahman, M. S., Khan, I. A., and Kummer, J. A. 2007. Widespread endocrine disruption and reproductive impairment in an estuarine fish population exposed to

seasonal hypoxia. Proceedings of the Royal Society B-Biological Sciences. 274: 2693-2702.

Thornton, K. W., and Lessem, A. S. 1978. A temperature algorithm for modifying biological rates. Transactions of the American Fisheries Society. 107: 284-287.

Thronson, A. and Quigg, A. 2008. Fifty-five years of fish kills in coastal Texas. Estuaries and Coasts. 31(4): 802-813.

Tyler, R. M. and Targett. 2007. Juvenile weakfish *Cynoscion regalis* distribution in relation to diel-cycling dissolved oxygen in an estuarine tributary. Marine Ecology Progress Series. 333: 257-269.

Videler, J. J. and Wardle, C. S. 1991. Fish swimming stride by stride: speed limits and endurance. Reviews in Fish Biology and Fisheries. 1:23-40.

Walker, N. D. and Rabalais, N. N. 2006. Relationships among satellite chlorophyll *a*, river inputs, and hypoxia on the Louisiana Continental Shelf, Gulf of Mexico. Estuaries and Coasts. 29(6B): 1081-1093.

Wang, L. and Justic, D. 2006. A modeling study of the physical processes affecting the development of seasonal hypoxia over the inner Louisiana-Texas shelf: circulation and stratification. Continental Shelf Reasearch. 29: 1464-1476.

Ware, D. M., and Thomson, R. E. 2005. Bottom-up ecosystem trophic dynamics determine fish production in the northeast Pacific. Science. 380: 1280-1284.

White, M. L. and Chittenden, M. E. Jr. 1977. Age determination, reproduction and population dynamics of the Atlantic croaker, *Micropogonias undulatus*. Fishery Bulletin. 75: 109-124.

Yakupzack, P. M., Herke, W. H., and Perry, W. G. 1977. Emigration of juvenile Atlantic croakers, Micropogon undulatus, from a semi-impounded marsh in southwestern Louisiana. Transaction of the American Fisheries Society. 106(6): 538-544.

APPENDIX A: DERIVATION OF THE MILD, INTERMEDIATE, AND SEVERE HYPOXIA MAPS

The extent and location of hypoxia under each scenario were determined analyzing by first processing a digital image of a map depicting the frequency of occurrence of hypoxia off the Louisiana Coast (http://www.gulfhypoxia.net) using the image function in MATLAB (2007b). The map showed the percent frequency (<25, 25-50, 50-75, >75) of all samples for 1985-2005 that had DO less than 2.0 mg/L. Using these four delineated subregions on the map, DO gradients in grid cells were then created by first assigning DO-multiplier values to the map: zero to points on the image map at the center of areas where hypoxia occurred greater than 75% of the time, 0.50 to the perimeters of the areas delineated as hypoxic 50-75% of the time, and 0.25 to the perimeters of areas delineated as hypoxic <25% of the time. DO values between 0 and 8 mg/L were then specified for every cell within the areas where seasonal hypoxia occurred by multiplying the DO-multipliers by 2 for the severe, 4 for the intermediate, and 8 for the mild scenarios to obtain DO values (0-4 mg/L) within the area where hypoxia occurs >50% of the time and then interpolating from the edge of the area where seasonal hypoxia occurs (DO = 8 mg/L) to the center of areas where hypoxia occurs >75% of the time (DO = 0 mg/L). For example, under the mild scenario the normalized values were multiplied by 8 so minimum DO values in areas where hypoxia occurs >75% and 50% of the time were $\leq$ 2.0 mg/L and $\leq$ 4.0 mg/L, respectively.

APPENDIX B: OVERVIEW OF THE BIOENERGETICS MODEL

The bioenergetics model used for Atlantic croaker in the NWGOM was based on Nye's (2008) model for Atlantic croaker in Chesapeake Bay. Nye (2008) used separate models for different size classes due to differences in the relationship between consumption or respiration and temperature. The temperature dependence function for consumption was calculated for all sizes using the Thorton and Lessem (1978) algorithm:

$$f(T) = K_a \cdot K_b$$

$$K_a = (ck1 \cdot L1)/\big(1 + ck1 \cdot (L1 - 1)\big)$$

$$L1 = e^{G1 \cdot (T - cq)}$$

$$G1 = (cto - cq)^{-1} \cdot ln\Big(\big(0.98 \cdot (1 - ck1)\big)/(ck1 \cdot 0.02)\Big)$$

$$K_b = (ck4 \cdot L2)/\big(1 + ck4 \cdot (L2 - 1)\big)$$

$$L2 = e^{G2 \cdot (ctl \cdot T)}$$

$$G2 = (cto - cq)^{-1} \cdot ln\Big(\big(0.98 \cdot (1 - ck1)\big)/(ck1 \cdot 0.02)\Big)$$

The temperature dependence function for respiration for individuals ≥ 9.0g followed a simple exponential relationship:

$$f(T) = e^{rq \cdot T}$$

For croaker < 9.0g, the temperature dependence function followed Kitchell et al.'s (1977) formulation:

$$f(T) = V^X \cdot e^{X \cdot (1 - V)}$$

$$V = (rtm - T)/(rtm - rto)$$

$$X = (Z^2 \cdot (1 + (1 + 40/Y)^{0.5})^2)/400$$

$$Z = ln(rq) \cdot (rtm - rto)$$

$$Y = ln(rq) \cdot (rtm - rto + 2)$$

VITA

Sean Creekmore was born in Nashville, Tennessee, in 1980. He graduated from Hume-Fogg Magnet High School in 1998. He enrolled at the University of West Florida in the fall of 2004, and received a Bachelor of Science in marine biology in the spring of 2007. He entered Louisiana State University in the fall of 2007 and began work on a Master of Science degree from the Department of Oceanography and Coastal Sciences.